

AD-A953012

AIR MINISTRY
For Official Use

R. & M. No. 1566

UNLIMITED

①

AERONAUTICAL RESEARCH COMMITTEE
-REPORTS AND MEMORANDA No. 1566
(T.3434)

Wind Tunnel Interference on Wings, Bodies and Airscrews

By H. GLAUERT
F.R.S.

Communicated by
THE DIRECTOR OF SCIENTIFIC RESEARCH, AIR MINISTRY

SEPTEMBER 1933
Crown Copyright Reserved

84 01 06 004

DTIC
SELECTED
JAN 06 1984
S E



COPYRIGHT ©
September 1933
CONTROLLER
HMSO LONDON

LONDON
PRINTED AND PUBLISHED BY HIS MAJESTY'S STATIONERY OFFICE
To be purchased directly from H.M. STATIONERY OFFICE at the following addresses:
Admiral House, Kingsway, London, W.C.2; 120, George Street, Edinburgh 2;
York Street, Manchester 1; 11, St. Andrew's Crescent, Cardiff

or through any Bookseller
1933

Price 4s. 6d. Net

This document has been approved
for public release and sale; its
distribution is unlimited.

23-1566

DTIC FILE COPY

WIND TUNNEL INTERFERENCE ON WINGS, BODIES AND AIRSCREWS

By H. GLAUERT, F.R.S.

Communicated by the Director of Scientific Research,
Air Ministry

Reports and Memoranda No. 1566

13th September, 1933*

Summary.—This report provides a comprehensive survey of the subject of wind tunnel interference on wings, bodies and airscrews. The basis of the theoretical treatment of the subject is examined critically and the method of analysing particular problems is explained in detail, but the reader is referred to the original papers for the more complex parts of the mathematical analysis. Experimental results are quoted to justify the theoretical formulae or to derive empirical values to complete the theoretical analysis. The results required for the practical application of the correction formulae are given in suitable tables and figures, and a full list of references is appended to the report, grouped according to the four main parts of the report and arranged chronologically in each group.

Accession For	NTIS GRA&I	<input checked="" type="checkbox"/>	<input type="checkbox"/>	<input type="checkbox"/>
	DTIC TAB	<input type="checkbox"/>	<input type="checkbox"/>	<input type="checkbox"/>
	Unannounced	<input type="checkbox"/>	<input type="checkbox"/>	<input type="checkbox"/>
	Justification	<input type="checkbox"/>	<input type="checkbox"/>	<input type="checkbox"/>
By				
Distribution/				
Availability Codes				
Avail and/or				
Special				
Pist				
	A-1			

UNANNOUNCED



* R.A.E. Report, June, 1933.

CONTENTS

Section	Page
1. General introduction	1
PART I	
<i>Wings, Three Dimensions</i>	
2. General discussion	3
3. Method of images	5
4. Interference flow	8
5. Closed tunnels and free jets	11
6. Circular tunnels	13
7. Effect of lift distribution	17
8. Plane walls	19
9. Rectangular tunnels	21
10. Elliptic tunnels	29
11. Downwash and tailsetting	35
12. Maximum lift coefficient	38
PART 2	
<i>Wings, Two Dimensions</i>	
13. Induced curvature of the flow	41
14. Free jets	46
15. Closed wind tunnels	48
PART 3	
<i>Symmetrical Bodies</i>	
16. General discussion	50
17. Two dimensions	52
18. Three dimensions	57
19. Pressure gradient	61
PART 4	
<i>Airscrews</i>	
20. General discussion	66
21. Closed wind tunnels	67
22. Free jets	70
23. Airscrew and body	71

WIND TUNNEL INTERFERENCE ON WINGS, BODIES
AND AIRSCREWS

By H. GLAUERT, F.R.S.

Communicated by the Director of Scientific Research,
Air Ministry

Reports and Memoranda No. 1566

13th September, 1933

1. *General Introduction.*—It is well known that the aerodynamic force experienced by a body may be seriously modified by the proximity of another body, even when there is no direct contact. The study of such interference is an important branch of aerodynamics, but in the first place it is necessary to know the behaviour of the body apart from any interference. The most convenient method of experiment is to investigate the behaviour of a model in the artificial stream of a wind tunnel, and the limited extent of this stream, bounded either by the rigid walls of a closed type of wind tunnel or by the free surface of an open jet, inevitably leads to some constraint of the flow and to some interference on the behaviour of the model. This interference could be minimised by using very small models, but it is desirable for many reasons that the model should be as large as possible. The study of wind tunnel interference is therefore of great importance, since some interference is inevitable, and an accurate knowledge of this interference will justify the use of larger models than would otherwise be permissible.

The general nature of the interference can be appreciated most readily by considering the conditions in a closed tunnel. If a large body is placed in the stream, the first and most obvious constraint imposed by the rigid walls of the tunnel is that the stream is unable to expand laterally as freely as it would in an unlimited fluid, and in consequence that the velocity of flow past the body is increased, leading to an intensification of the forces experienced by the body. Another choking constraint of a different character arises if there is a wake of reduced or increased velocity behind the body, as occurs respectively with a bluff body or an airscrew. The necessity of maintaining continuity of flow in the tunnel then implies that the velocity and pressure of the stream surrounding the wake

will differ from the undisturbed values far in front of the body, and this change of pressure reacts back to cause a change in the force experienced by the body. The interference experienced by a lifting body, such as a wing, is of a different character. The lift of a wing is associated with a general downward movement of the air behind the wing, and the constraint of the tunnel walls on this downwash modifies the behaviour and aerodynamic characteristics of the wing. Finally a fourth type of interference occurs if there is a gradient of static pressure down the stream of the wind tunnel. This pressure gradient arises owing to the development of the frictional boundary layer of reduced velocity along the walls of the tunnel, which leads to an increase of velocity and a decrease of pressure along the axis of the tunnel. Any body is therefore tested in a slightly convergent stream, and experiences an increased drag owing to the drop of static pressure from nose to tail.

These various interference effects in a closed tunnel, together with the corresponding effects in a free jet, will be discussed in detail for different types of body, which can be grouped conveniently under the headings of wings, symmetrical bodies and airscrews, but before proceeding to this analysis it is desirable to consider the precise nature of the boundary conditions, and the limitations of the theoretical treatment of the subject.

The pressure gradient correction will be reserved for special consideration in Section 19 of Part 3, since it is important only for bodies of low drag and may be neglected in the consideration of wings and airscrews. Moreover, the pressure gradient, which is due in a closed tunnel to the development of the frictional boundary layer along the walls and to leakage through the walls, can be eliminated by designing the wind tunnel with a slight expansion in the direction of the stream, and is sensibly zero in a free jet. The discussion of the other types of tunnel interference is based on the conception of an ideal stream without any pressure gradient along its axis, and neglects both the boundary layer along the walls of a closed tunnel and the analogous disturbed region at the boundary of a free jet where the stream mingles with and draws along some of the surrounding air.

The boundary condition at any wall of a closed tunnel is expressed precisely by the condition that the normal component of the fluid velocity must be zero. The corresponding condition for a free jet is that the pressure at the boundary must have a constant value, equal to the pressure of the surrounding air, but it is in practice impossible to use this exact condition in the analysis owing to the distortion of the shape of the jet caused by the presence of a body in the stream. The approximation is therefore adopted of applying this condition of constant pressure at the undisturbed position of the boundary of the jet. As an additional approximation, which is of the same order of accuracy as the previous one, it is assumed that the disturbance to the tunnel velocity V at the boundary

of the jet is small. If (u, v, w) are the components of the disturbance, the pressure p at the boundary of the jet is obtained from Bernoulli's equation as

$$\begin{aligned} p &= p_0 + \frac{1}{2} \rho V^2 - \frac{1}{2} \rho \{(V + u)^2 + v^2 + w^2\} \\ &= p_0 - \rho V u - \frac{1}{2} \rho (u^2 + v^2 + w^2) \dots \dots \dots (1.1) \end{aligned}$$

and to the first order of the disturbance the condition of constant pressure is simply that u is constant. But u is evidently zero far in front of the body in the undisturbed stream, and hence u must be zero at all points of the boundary. This implies that the velocity potential ϕ , which represents the change of flow from the uniform undisturbed stream, must have a constant value over the whole boundary of the free jet, and the boundary conditions assumed in the analysis are now simply:—

$$\left. \begin{array}{l} \text{Closed tunnel} \quad \frac{\partial \phi}{\partial n} = 0 \\ \text{Free jet} \quad \phi = \text{constant} \end{array} \right\} \dots \dots (1.2)$$

The boundary condition for a closed tunnel is exact and precise, except for any effects due to the frictional boundary layer along the walls. The boundary condition for a free jet is approximate only, being applied at the undisturbed position of the boundary and based on the assumption of small disturbing velocities. There is also one other point in which the treatment of a closed tunnel is more precise than that of a free jet. A closed tunnel usually extends for a considerable length with constant cross-section before and behind the model, whereas a free jet usually issues from a closed cylindrical mouth immediately in front of the model and is received into a collector at a moderate distance behind the model. Thus the conditions differ appreciably from those of the long free jet, envisaged in the analytical treatment of the subject, and the validity of the theoretical interference corrections must rest ultimately on experimental confirmation of their accuracy.

PART I

Wings, Three Dimensions

2. *General discussion.*—The method of analysing the interference experienced by a wing in a closed tunnel or in a free jet is due to Prandtl¹. The nature of the boundary conditions and the approximate assumptions made regarding these conditions for a free jet have been discussed previously in Section 1, but in the development of the analysis it is necessary to make some further assumptions regarding the flow past the wing itself. The lift of the wing is intimately related to the circulation of the flow round the wing, and in effect the wing can be regarded as a group of bound vortices running along its span. In general the lift and circulation have

their maximum values at the centre of the wing and fall off gradually to zero at the wing tips. This lateral decrease of circulation from the centre of the wing outwards is accompanied by the creation of free trailing vortices which spring from the trailing edge of the wing and pass down stream. These trailing vortices are deflected downwards with the general downwash behind the wing, and, since a vortex sheet is unstable, they ultimately roll up into two vortices somewhat inboard of the wing tips. In the development of aerofoil theory, however, these effects are ignored and the trailing vortices are assumed to lie along straight lines passing downstream from the wing. This same assumption is made in the analysis of wind tunnel interference, and the analysis is therefore strictly applicable only to lightly loaded wings.

The problem of a wing in a small tunnel involves motion in three dimensions, but Prandtl¹ has shown that it can conveniently be reduced to a problem in two dimensions only, when the wing is regarded as a lifting line extending from wing tip to wing tip. Considering first the flow past the wing in an unlimited fluid and taking the x co-ordinate downstream, the velocity potential, due to the wing and additional to that of the undisturbed stream, is of the form

$$\phi = f(y, z) + F(x, y, z) \quad \dots \quad (2.1)$$

where the first function represents the velocity potential in the transverse plane containing the wing and the second function changes sign with x . Since ϕ must be zero far in front of the wing, it follows that far behind the wing the velocity potential will have the value

$$\phi_{\infty} = 2f(y, z) \quad \dots \quad (2.2)$$

Turning now to the problem of a wing in a free jet, the interference due to the limited extent of the stream will be represented by the addition of a term ϕ' to the velocity potential, which must satisfy the conditions that ϕ' is finite at all points in the limited stream and that $(\phi + \phi')$ must be zero at all points of the boundary. It follows that ϕ' can be divided into two terms of the same form as ϕ , and that its value in the ultimate wake will be double its value at the corresponding point in the transverse plane containing the wing. The interference experienced by the wing depends solely on the flow in this transverse plane, and hence as a convenient method of analysis it suffices to analyse the flow in a transverse plane of the distant wake, which is simply a two-dimensional problem, and to deduce that the interference experienced by the wing is half that which occurs in the distant wake. A similar argument can be applied to the problem of a closed wind tunnel where the boundary condition is now

$$\frac{\partial \phi}{\partial n} + \frac{\partial \phi'}{\partial n} = 0 \quad \dots \quad (2.3)$$

and it is again possible to reduce the problem to that of two-dimensional flow in a transverse plane of the distant wake.

The interference due to the limited extent of the stream will in general modify the distribution of lift across the span of the wing and in an exact analysis of the problem it would be necessary to take due account of this effect. This aspect of the problem is discussed in Section 7 below, but unless the span of the wing is a very large fraction of the width of the tunnel the resulting change of lift distribution is very small and may be neglected. Generally it suffices to assume that the lift is distributed elliptically across the span, as on a wing of elliptic plan form, and often it is possible to proceed to the even simpler approximation of uniform distribution of lift across the span of the wing. When the span of the wing is a very small fraction of the width of the tunnel, the form assumed for the lift distribution is quite immaterial and it then suffices to assume that the total lift force of the wing is concentrated at the centre of its span and to calculate the interference at this single point. This type of solution will subsequently be referred to as that applicable to small wings.

3. Method of images.—The conception of images, as used in aerodynamical problems, can be appreciated by considering a few simple examples. If two aeroplanes are flying horizontally side by side there will evidently be no flow across the vertical plane of symmetry midway between the aeroplanes, and this plane could be replaced by a rigid wall without altering the flow in any way. Thus the problem of an aeroplane flying parallel to a vertical wall can be solved by introducing the image aeroplane on the other side of the wall and by considering the new problem of the two aeroplanes flying side by side. Similarly the interference experienced by an aeroplane flying close to the ground can be solved by introducing the inverted image aeroplane below the ground. This method of introducing the appropriate image or set of images to represent the constraint of the boundary of the stream is capable of very wide application, and is the method used for analysing most problems of wind tunnel interference.

The discussion of Section 2 has shown that the problem of the interference experienced by a wing in a closed tunnel or in a free jet can be solved by considering the transverse flow in a section of the distant wake. In this plane the wing is represented solely by the system of its trailing vortices, which now appear as point vortices and extend along a line of length equal to the span of the wing, and the problem to be solved is the determination of the flow which must be superimposed on that due to the vortices in order to satisfy the appropriate condition at the boundary of the stream. In the simple assumption of a wing of uniform loading across the span the vortex systems comprise merely two point vortices of equal and opposite strengths at a distance apart equal

to the span of the wing. More generally any wing can be represented by a distribution of such pairs of vortices extending across the whole span, and hence the problem of a wing with any type of lift distribution across its span can be derived from the simpler problem of a uniformly loaded wing by a process of integration.

The method of images can be used directly when the cross-section of the boundary of the stream is rectangular or circular, and solutions for some other forms can be derived from these primary solutions by means of suitable conformal transformations. The form of image required in a single rectilinear boundary is illustrated in Fig. 1. The image of a single vortex in a rigid rectilinear boundary is an equal vortex of opposite sign (Fig. 1a), since this pair of vortices will by symmetry give zero normal velocity at the boundary. Each vortex will give the same component of velocity parallel to the boundary, and hence the condition of zero flow along a free boundary can be obtained by reversing the sign of the image (Fig. 1b), and vortex and image have now the same sign. Thus the image system for a free boundary can be derived from that for a rigid boundary by reversing the sign of the images. The image system of a uniformly loaded wing in the presence of a rigid vertical wall is shown in Fig. 1c, and the corresponding system for a horizontal boundary in Fig. 1d. Here, and generally throughout the report, it is assumed that the span of the wing is horizontal. The image in the vertical wall is a replica of the wing itself, but the image in the horizontal wall is an inverted wing. By applying the fundamental conceptions illustrated in Fig. 1 it is possible to build up the image system required for a pair of walls or for any rectangular boundary. These problems usually involve infinite series of images and examples of such systems will be discussed later in the report.

A circular boundary (Fig. 2) can also be represented quite simply by the method of images. Considering first a rigid boundary, the image of a point vortex of strength K at any point A is an equal and opposite point vortex at the inverse point A' . The stream function ψ at any point P due to these two point vortices is simply

$$\psi = \frac{K}{2\pi} \log \frac{A'P}{AP}$$

since the complex potential function of a point vortex of strength K and anti-clockwise rotation at the point z_0 is

$$\phi + i\psi = -\frac{iK}{2\pi} \log(z - z_0) \quad \dots \quad (3.1)$$

Now if P is a point of the circular boundary, the triangles OAP and OPA' are similar, and hence

$$\frac{A'P}{AP} = \frac{OP}{OA} = \text{const.}$$

which proves that the circular boundary is a streamline of the flow and may therefore be regarded as a rigid boundary.

By analogy with the problem of a rectilinear boundary we might anticipate that the same image could be used for a free boundary if the sign of the image were reversed. The velocity potential of the vortex at A and of an equal image at A' is, apart from the addition of any arbitrary constant,

$$\phi = \frac{K}{2\pi} (R\dot{A}P + R\dot{A}'P)$$

and since

$$\begin{aligned} R\dot{A}'P &= A\dot{O}P + \dot{O}P\dot{A}' \\ &= A\dot{O}P + \dot{O}A\dot{P} \end{aligned}$$

we obtain

$$\phi = \frac{K}{2\pi} (\pi + \theta - \alpha)$$

where θ denotes the angular position of the radius OP . Thus the velocity potential of the vortex and its image is not constant along the circumference of the circle and the necessary condition for a free boundary is not satisfied. If, however, we introduce a second vortex of equal and opposite strength at any other point inside the circle, the velocity potential of this second vortex and its image will be of the form

$$\phi = -\frac{K}{2\pi} (\pi + \theta - \beta)$$

and on addition to the previous expression the variable term θ disappears. Thus the necessary condition for a free boundary is satisfied by a pair of vortices anywhere inside the circle and by the corresponding images. Since the vortices representing a wing always occur in pairs of this kind, the method of images can be used for a free circular boundary. The image system is identical, except for the change of sign of the vorticity, with the system for a rigid boundary.

A wing with uniform distribution of lift across its span is represented by a pair of vortices at its tips, and any form of lift distribution can be represented by a system of pairs of vortices distributed along the span of the wing. Thus the conditions for any arbitrary distribution of lift can be derived by integration from the simpler condition of a wing with uniform distribution of lift across its span. In general the lift distribution is symmetrical about the centre of the wing. Take the origin O at the centre of the wing and the axis Ox to starboard along the span. If Γ is the circulation at any

point x of the wing, the strength of the trailing vortex springing from an element δx of the wing is simply

$$K = -\frac{d\Gamma}{dx} \delta x \dots \dots (3.2)$$

and the lift of the wing is

$$L = \int_{-s}^s \rho V \Gamma dx \dots \dots (3.3)$$

With uniform loading we obtain simply a pair of trailing vortices of strength $\pm \Gamma$ and the lift of the wing is

$$L = 2s \rho V \Gamma \dots \dots (3.4)$$

Occasionally it is convenient to assume that the span of the wing is extremely small, or in other words that the lift is concentrated at the centre of the wing. The pair of vortices then join to form a doublet of strength

$$\mu = 2s \Gamma$$

and by virtue of equation (3.4)

$$\mu = \frac{L}{\rho V} \dots \dots (3.5)$$

For future reference it may be noted that the complex velocity potential of a doublet, which is the limit of a positive vortex at $x = s$ and a negative vortex at $x = -s$, is

$$\phi + i\psi = \frac{i\mu}{2\pi z} \dots \dots (3.6)$$

4. Interference flow.—The transverse flow in a plane, normal to the direction of motion and far behind a wing moving in an unlimited fluid, is that due to the system of trailing vortices, and the calculation of this flow is the basis of the standard theory of the induced drag of a wing. When the stream is limited by rigid or free boundaries there is a constraint of the flow and the change in the induced velocity at any point of the sheet of point vortices is a measure of the interference experienced by the wing due to the tunnel constraint. In these problems where the necessary boundary condition can be satisfied by the introduction of a set of images, the tunnel interference can be calculated as the effect of the induced velocities of this set of images.

Consider, as an example, a wing with uniform lift distribution across its span, lying along a diameter of a closed circular tunnel of radius a (Fig. 3). Take the origin of coordinates at the centre of the wing and of the tunnel, the x axis along the span and the y axis normal to it. There will be two trailing vortices, one of strength K at the point $A(x = s)$ and the other of strength $-K$ at

$B(x = -s)$. The image vortices occur at the inverse points and are $-K$ at A' ($x = a^2/s$) and K at B' ($x = -a^2/s$). At any point of the line AB there is an upward induced velocity due to the images, of magnitude

$$v = \frac{K}{2\pi} \left\{ \frac{1}{\frac{a^2}{s} - x} + \frac{1}{\frac{a^2}{s} + x} \right\} \\ = \frac{K}{2\pi} \cdot \frac{2sa^2}{a^4 - s^2x^2} \dots \dots (4.1)$$

and at the midpoint O we have simply

$$v_0 = \frac{Ks}{\pi a^2}$$

This expression represents the induced velocity in the wake and is double that experienced by the wing itself. Also the lift of the wing is

$$L = 2s \rho VK$$

and hence the induced velocity at the centre of the wing is

$$v_0 = \frac{Ks}{2\pi a^2} = \frac{L}{4\pi a^2 \rho V} \dots \dots (4.2)$$

The induced velocity varies across the span of the wing and would also be modified if due allowance were made for the actual lift distribution of the wing, but this simple example serves to illustrate the nature of the tunnel interference and the form of the results. The induced velocity is proportional to the lift of the wing and inversely proportional to the area of cross-section of the tunnel. In a closed tunnel a wing usually experiences an upwash and in consequence, at a given angle of incidence relative to the undisturbed stream, the lift of the wing is increased and its line of action is inclined forwards. It is however more convenient to make the comparison of free and constrained conditions on the basis of equal lift in the tunnel and in free flow. Thus in general, at a given value of the lift coefficient, the angle of incidence and the drag coefficient in a closed tunnel will be lower than in free flow. In an open jet the sign of the interference is changed, and the measured angle of incidence and drag coefficient are too high.

Throughout the subsequent analysis, unless otherwise stated, the following notation and conventions will be used. The origin O will be at the centre of the wing, which in turn will in general be assumed to be at the centre of the tunnel. The axis of x will be taken along the span to starboard and the axis of y upwards in the direction of the observed lift force. The upward induced velocity at any point of the wing will be denoted by v . This velocity is

exactly half that calculated from the image vortices of the wake, and may be obtained directly by using a factor 4π instead of 2π in the standard hydrodynamical formula

$$q = \frac{K}{2\pi r}$$

which gives the velocity q at a distance r from a point vortex of strength K in two-dimensional motion.

Due to the upward induced velocity v the line of action of the lift force on the element of wing is inclined forwards by the angle v/V , and hence the reduction of drag in the tunnel or the correction which must be applied to the observed value is

$$\Delta D = \int \frac{v}{V} dL \quad \dots \quad (4.3)$$

The correction to the angle of incidence strictly involves a twisting of the wing in order to maintain the same distribution of lift across the span in the tunnel as in free air, but this twisting can be neglected in general and the correction to the angle of incidence may be taken to be

$$\Delta \alpha = \frac{1}{L} \int \frac{v}{V} dL \quad \dots \quad (4.4)$$

In order to obtain a non-dimensional representation of the results the induced velocity v will be expressed in the form

$$\frac{v}{V} = \eta \frac{L}{C \bar{v}^2} = \eta \frac{S}{C} k_L \quad \dots \quad (4.5)$$

where C is the area of cross-section of the tunnel. The value of η will in general be a function of x/s , and its mean value, weighted according to the distribution of lift across the span, is

$$\bar{\eta} = \frac{1}{L} \int \eta dL \quad \dots \quad (4.6)$$

The values of η and $\bar{\eta}$ can be calculated in different ways, depending on the assumptions made regarding the lift distribution and on the approximations made regarding the system of images. The corrections to the observed values of the angle of incidence and drag coefficient will be expressed as—

$$\Delta \alpha = \delta \frac{S}{C} k_L \quad \dots \quad (4.7)$$

and

$$\Delta k_D = \delta \frac{S}{C} k_L^2 \quad \dots \quad (4.8)$$

Thus δ represents the magnitude of the tunnel constraint and in general, as will be seen later, δ may be taken to be the value of $\bar{\eta}$ calculated on the assumption of elliptic distribution of lift across the span of the wing. The value of δ is usually positive for a closed tunnel and negative for a free jet.

5. *Closed tunnels and free jets.*—The discussion of the two previous sections has shown that the image systems for any wing in a closed circular tunnel and for the same wing in the same position in a free circular jet are identical except for a change of sign of all the image vortices, and hence that the interference experienced by the wing is of the same magnitude but of opposite sign in the two types of wind tunnel. This simple relationship is a special property of the circular cross-section, but it is possible to establish an interesting general theorem¹⁵ for small wings in any wind tunnel.

Consider any shape of tunnel, as shown in Fig. 4, and any position of the wing. Take the origin of co-ordinates at the centre of the wing, with Ox along the span and Oy in the direction of the lift. The velocity field due to a very small wing in this position is that due to a doublet of strength μ at O , directed along the negative branch of the y axis, and the complex potential function of the flow is

$$\phi + i\psi = \frac{i\mu}{2\pi z} = \frac{\mu(y + ix)}{2\pi r^2} \quad \dots \quad (5.1)$$

Now consider a closed boundary and assume the region outside the boundary to be filled with fluid at rest. The rigid boundary can then be replaced by a vortex sheet of strength k per unit length, such that the normal velocity at any point of the boundary, due to this vortex sheet and to the doublet at the origin, is zero. If ds and δn are respectively elements of the boundary and of the inward normal at any point P of the boundary, the normal component of the velocity due to the doublet is

$$q_n = \frac{\partial}{\partial n} \left(\frac{\mu y}{2\pi r^2} \right) - \frac{\partial}{\partial s} \left(\frac{\mu x}{2\pi r^2} \right) \quad \dots \quad (5.2)$$

Also if R is the distance of any other point Q of the boundary from P and if (n, R) denotes the angle between PQ and the normal at P , the necessary boundary condition is

$$\int \frac{k}{2\pi r} \sin(n, R) ds = q_n \quad \dots \quad (5.3)$$

The interference experienced by the wing due to the constraint of the boundary is the component of the velocity due to the vortex sheet parallel to the axis of y , and this velocity is

$$v = - \int \frac{k}{2\pi r} \cos \theta ds \quad \dots \quad (5.4)$$

Consider next a tunnel of the same shape with a free boundary, on which the necessary boundary condition is that the velocity potential ϕ has a constant value or that the tangential component of the velocity is zero. Let the small wing still be situated at the origin O , but rotate it through a right angle so that its span lies along Oy and its lift is in the direction Ox . The complex potential function of the flow due to the wing is then

$$\phi + i\psi = \frac{\mu}{2\pi z} = \frac{\mu(x - iy)}{2\pi r^2} \quad \dots \quad (5.5)$$

and the tangential component of the velocity at P due to the wing is

$$q_s = \frac{\partial}{\partial s} \left(\frac{\mu x}{2\pi r^2} \right) = - \frac{\partial}{\partial n} \left(\frac{\mu y}{2\pi r^2} \right) \quad \dots \quad (5.6)$$

The necessary boundary condition can be satisfied by assuming along the boundary a distribution of sources of strength m per unit length such that the tangential component of the velocity at the boundary due to these sources exactly balances that due to the wing. The necessary condition is

$$\int \frac{m}{2\pi r} \sin(n, R) ds = q_s \quad \dots \quad (5.7)$$

and the corresponding interference experienced by the wing is the velocity

$$u = - \int \frac{m}{2\pi r} \cos \theta ds \quad \dots \quad (5.8)$$

A comparison of corresponding pairs of equations for the rigid and free boundaries indicates that

$$\begin{aligned} q_s &= -q_n \\ m &= -k \end{aligned}$$

and hence that

$$u = -v \quad \dots \quad (5.9)$$

Thus it has been proved that the interference on a very small wing in a tunnel with a free boundary is of the same magnitude, but of opposite sign, as that on the same wing, rotated through a right angle, in a tunnel of the same shape with a rigid boundary. In practical applications the wing is generally situated at the centre of the tunnel, and the tunnel itself is symmetrical in shape about the co-ordinate axes (e.g., rectangle or ellipse). The general theorem then states that the interference on a small wing at the centre of an open symmetrical tunnel, of breadth b parallel to the span and of height h , is of the same magnitude but of opposite sign as that on

the same wing in closed tunnel of breadth h and height b . The theorem is strictly true for very small wings only, but it will also be approximately true for wings of moderate size.

6. *Circular tunnels.*—The formulae for the interference experienced by a wing in a circular tunnel are due to Prandtl¹ and have been expressed in concise forms by Rosenhead¹¹. The system of images required to represent the constraint of the boundary, whether of the closed or free type, has been discussed in some detail in Section 3, and it has been demonstrated that the interference experienced by any wing in a free circular jet is identical, except for a change of sign, with that experienced by the same wing in a closed circular tunnel of the same diameter. It will suffice, therefore, to consider the conditions in a closed tunnel.

The image system for a wing with uniform distribution of lift across its span is shown in Fig. 3, and the normal induced velocity at any point of the wing is

$$v = \frac{K}{4\pi} \left\{ \frac{1}{\frac{a^2}{s} - x} + \frac{1}{\frac{a^2}{s} + x} \right\} = \frac{sa^2 K}{2\pi(a^4 - s^2x^2)}$$

Writing for convenience

$$\begin{aligned} \xi &= \frac{sx}{a^2} \\ \zeta &= \frac{s^2}{a^2} \end{aligned} \quad \dots \quad (6.1)$$

we have

$$v = \frac{sK}{2C(1 - \xi^2)} \quad \dots \quad (6.2)$$

which indicates that the induced velocity has its minimum value at the centre of the wing and increases outwards along the span.

Remembering that

$$L = 2s \rho VK$$

or

$$VS k_L = 2s K$$

the expression for the coefficient η of the induced velocity, defined by equation (4.5), becomes

$$\begin{aligned} \eta &= \frac{1}{4} (1 - \xi^2)^{-1} \\ &= \frac{1}{4} (1 + \xi^2 + \xi^4 + \dots) \quad \dots \quad (6.3) \end{aligned}$$

and the mean value of this coefficient taken across the span of the wing is

$$\begin{aligned} \bar{\eta} &= \frac{1}{\zeta} \int_0^{\zeta} \eta d\xi \\ &= \frac{1}{8\zeta} \log \frac{1+\zeta}{1-\zeta} \\ &= \frac{1}{4} \left(1 + \frac{1}{3} \zeta^2 + \frac{1}{5} \zeta^4 + \dots \right) \dots \dots (6.4) \end{aligned}$$

In order to proceed to the calculation of the interference experienced by a wing with elliptic distribution of lift across its span, it is necessary to replace s in the formula (6.2) by a current co-ordinate x_1 , to take

$$K = -\frac{d\Gamma}{dx_1} dx_1$$

where Γ is the circulation round the wing, and to integrate with respect to x_1 from 0 to s . The circulation Γ is of the form

$$\Gamma = \Gamma_0 \frac{\sqrt{s^2 - x_1^2}}{s} \dots \dots \dots (6.5)$$

and the lift of the wing is now

$$L = \int_{-s}^s \rho V \Gamma dx_1 = \frac{\pi}{2} s \rho V \Gamma_0$$

or

$$VS k_L = \frac{\pi}{2} s \Gamma_0 \dots \dots \dots (6.6)$$

Thus for a wing with elliptic loading

$$v = \int_0^s \frac{\Gamma_0 a^4 x_1^2 dx_1}{2sC(a^4 - x^2 x_1^2) \sqrt{s^2 - x_1^2}}$$

and converting to the non-dimensional system

$$\eta = \frac{1}{\pi} \int_0^{\zeta} \frac{\xi_1^2 d\xi_1}{(\zeta^2 - \xi^2 \xi_1^2) \sqrt{\zeta^2 - \xi_1^2}}$$

This integral can be evaluated by means of the substitutions

$$\begin{aligned} \xi_1 &= \zeta \sin \theta \\ \xi &= \tan \theta \end{aligned}$$

and we obtain

$$\begin{aligned} \eta &= \frac{1}{\pi} \int_0^{\frac{\pi}{2}} \frac{\sin^2 \theta d\theta}{1 - \xi^2 \sin^2 \theta} \\ &= \frac{1}{\pi \xi^2} \int_0^{\frac{\pi}{2}} \left(\frac{1}{1 - \xi^2 \sin^2 \theta} - 1 \right) d\theta \\ &= \frac{1}{\pi \xi^2} \left\{ \int_0^{\frac{\pi}{2}} \frac{d\theta}{1 + (1 - \xi^2) \theta^2} - \frac{\pi}{2} \right\} \end{aligned}$$

or finally

$$\begin{aligned} \eta &= \frac{1}{2\xi^2} \left((1 - \xi^2)^{-1} - 1 \right) \\ &= \frac{1}{4} \left(1 + \frac{3}{4} \xi^2 + \frac{5}{8} \xi^4 + \frac{35}{64} \xi^6 + \dots \right) \dots (6.7) \end{aligned}$$

The denominator of the coefficient of ξ^4 was given incorrectly as 128 in Prandtl's original paper¹ and has been repeated in other papers. The error was corrected by Rosenhead¹¹.

The mean value of η across the span, weighted according to the elliptic distribution of lift, is

$$\begin{aligned} \bar{\eta} &= \frac{4}{\pi} \int_0^{\frac{\pi}{2}} \eta \frac{\sqrt{s^2 - x^2}}{s^2} dx \\ &= \frac{4}{\pi \zeta^2} \int_0^{\zeta} \eta \sqrt{\zeta^2 - \xi^2} d\xi \end{aligned}$$

and after integration

$$\bar{\eta} = \frac{1}{4} \left(1 + \frac{3}{16} \zeta^2 + \frac{5}{64} \zeta^4 + \frac{175}{4096} \zeta^6 + \dots \right) \dots (6.8)$$

Numerical values of the coefficient $\bar{\eta}$ for uniform and for elliptic loading, deduced from the formulae (6.4) and (6.8), are given in Table 1, and it appears that the increase of $\bar{\eta}$ with the span of the wing is more rapid for uniform than for elliptic loading. The subsequent discussion of Section 7 indicates that in general the value of δ , required in the correction formulae (4.7) and (4.8), should be taken to be the value of $\bar{\eta}$ derived from the assumption of elliptic

TABLE 1

Values of $\bar{\eta}$ in a closed circular tunnel

Span/Diameter	..	0	0.2	0.4	0.6	0.8
Elliptic loading	..	0.250	0.250	0.251	0.256	0.273
Uniform loading	..	0.250	0.250	0.252	0.261	0.296

loading, since the lift distribution of a wing of conventional planform usually approximates to the elliptical form. Fig. 5 shows the variation of δ with the ratio of the wing span to the tunnel diameter, and the broken curve shows the values which would be deduced from the assumption of uniform loading. For a small wing δ has the value 0.250, and an examination of Table 1 or Fig. 5 indicates that the adoption of values of δ , based on the assumption of uniform loading, will lead to errors of the same magnitude as the simpler assumption of the value 0.250 appropriate to small wings.

As regards the accuracy required in the determination of the value of δ in the correction formulae, it may be noted that the value of the ratio S/C is usually less than 0.1 and that a value of 0.2 may be regarded as an extreme upper limit. Even in this extreme case an error of 0.025 in the value of δ produces errors of only 0.15 deg. in the angle of incidence and 0.0012 in the drag coefficient at a lift coefficient of 0.5. In general it will suffice to know the value of δ with an accuracy of ± 0.025 , and more accurate values are required only for unusually large values of the ratio S/C or of the lift coefficient of the wing. On this basis the value of δ for a closed circular tunnel can be taken to be 0.250, as for a small wing, unless the span or area of the wing is unduly large.

Experimental checks on the theoretical correction formulae have been obtained in both closed tunnels and free jets. Higgins⁷ tested two series of wings in a closed circular tunnel. The wings of the first series were of constant chord and varying span, so that the tunnel constraint was obtained only as a small modification to the correction for aspect ratio, but the second series comprised three wings of aspect ratio 6, tested at the same value of the Reynolds number, and thus gave a direct measure of the tunnel constraint. After trying several empirical corrections with little success, Higgins concluded that the theoretical formulae gave the best results. The largest value of the span-diameter ratio in these tests was 0.6, and the correction formulae for small wings ($\delta = 0.250$) were used in the analysis of the results.

Experiments in a free jet have been made at Göttingen⁴, using a series of five rectangular wings of the same aerofoil section and of the same aspect ratio. The span-diameter ratio ranged from 0.27 to 0.80 and the tests were made at a constant value of the Reynolds number. The observed polar curves (drag against lift) of the five wings showed systematic differences, but after correction for the tunnel constraint, using the values of δ appropriate to the span-diameter ratio for each wing, all the results fell on a single curve with the exception of those for the largest wing, where the theoretical formula appeared to underestimate the correction slightly. The lift curves (lift against incidence) showed similar characteristics, but the final agreement was not quite so good and the theoretical formula appears to underestimate slightly the necessary correction even for moderate values of the span-diameter ratio. This

discrepancy is ascribed to the influence of a general curvature of the jet, due to the lift of the wing, which is equivalent to a reduction of the effective camber of the wing section.

These conclusions are confirmed by some experiments of Knight and Harris¹⁰ with three wings of aspect ratio 5 and of span-diameter ratio 0.45, 0.60 and 0.75 respectively. The experiments were made in a free circular jet at a constant value of the Reynolds number, and, instead of correcting the results to free air conditions by means of the theoretical formulae, the observed values were analysed to deduce the appropriate value of δ for each wing.

TABLE 2
Free Circular Jet

Span/Diameter	0.45	0.60	0.75
Theoretical	0.252	0.256	0.266
From drag coefficient	0.250	0.254	0.284
From angle of incidence	0.254	0.264	0.354

Values of δ , ignoring the negative sign appropriate to a free jet, are given in Table 2, and it will be seen that they fully confirm the conclusions drawn from the earlier experiments at Göttingen. In view, however, of the previous remarks regarding the accuracy required in the value of δ , it appears that the deviation from the theoretical values does not become appreciable until the span of the wing exceeds two-thirds of the diameter of the tunnel.

7. *Effect of lift distribution.*—The interference experienced by a wing in a wind tunnel depends not only on the shape and size of the tunnel, but also on the type of distribution of lift across the span of the wing. In his original paper Prandtl¹ tried the alternative assumptions of uniform and elliptic distributions, and found that the first term of the series for δ had the same value in both cases. The results for a wing with uniform or with elliptic loading in a circular tunnel are given by equations (6.4) and (6.8) respectively. The first terms, which are identical, represent the interference which would be deduced from the assumption of a small wing with the total lift concentrated at its mid-point, and the subsequent terms represent the effect of the finite span of the wing, differing according to the assumed lift distribution. Thus in order to obtain a first approximation to the interference it suffices to consider a small wing and to calculate the induced velocity at its midpoint. This conclusion has also been verified for plane boundaries², and it appears that the first approximation is sufficiently accurate for most purposes unless the wing span exceeds 60 per cent. of the width of the tunnel.

In the discussion of circular tunnels results were derived for wings of any span with uniform or with elliptic loading, but this method of proceeding to a more accurate estimate of the tunnel interference is not strictly sound. The analysis compares two wings with the same loading in free air and in the tunnel, but in fact the induced velocity varies across the span of the wing, as shown by equation (6.7), and hence an untwisted wing in free air must be twisted in the tunnel in order to maintain the same lift distribution, whereas the practical problem is the determination of the change of the characteristics of the same wing in free air and in the tunnel. The effect of the twist necessary to maintain the same lift distribution appears to be of the same order of magnitude as the correction to the tunnel interference due to the variation of the induced velocity across the span of the wing, and hence it is necessary to consider the change of the lift distribution in passing from the tunnel to free air conditions.

The exact solution of this problem in a circular tunnel has been obtained by the present author¹⁵ and independently by Millikan¹⁶. The method of analysis adopted by both authors was to express the lift distribution by a suitable Fourier series with unknown coefficients, to calculate the corresponding induced velocity at any point of the wing, and then to determine the coefficients of the series to satisfy the conditions imposed by the shape of the wing. From this analysis it appeared that there is surprisingly little distortion of the lift distribution of an elliptic wing due to the tunnel constraint, even when the span of the wing was equal to the diameter of the tunnel, and that the modification to Prandtl's formula (6.8) for the interference experienced by a wing with elliptic loading was negligibly small. The application of the analysis to a rectangular wing¹⁵ led to similar conclusions, and it appears therefore that the interference formulae derived from the assumption of elliptic distribution of lift are sufficiently accurate for wings of elliptic and rectangular plan forms, whereas formulae derived from the assumption of uniform distribution of lift may be definitely misleading.

In view of this analysis and of the conclusions drawn from it, the interference experienced by any wing in a tunnel of any shape will be derived either as a first approximation on the assumption of a small wing with the total lift concentrated at its mid point, or as a closer approximation on the assumption of a wing of finite span with elliptic distribution of lift. This course should lead to reliable estimates of the tunnel interference experienced by wings of any shape or size, though some reconsideration may be necessary if the span of the wing is unduly large since, for example, the lift distribution on a rectangular wing must tend towards the uniform type in a closed rectangular tunnel when the span is nearly equal to the breadth of the tunnel.

8. *Plane walls.*—Throughout the subsequent discussion it will be assumed that the span of the wing is horizontal and that its lift is directed upwards. As explained previously in Section 3, a single vertical wall at the side of a wing then represents the condition of two aeroplanes flying side by side, and a single horizontal wall below the wing represents the condition of an aeroplane flying close to the ground. These problems, which have their own importance, will be examined here as an introduction to the problem of a rectangular wind tunnel, and as a second step it is convenient to consider the effect of two walls, vertical or horizontal, on opposite sides of the wing. Since, however, the results have no practical value in connection with tunnel interference, it will suffice to consider the problem of small wings only. The lift of the wing is concentrated at its mid-point and the flow induced by the wing is that of a doublet of strength

$$\mu = \frac{L}{\rho V} = VS k_L \dots \dots \dots (8.1)$$

as given previously in equation (3.5). In the figures representing the system of images, appropriate to any given boundaries, it will then be convenient to represent the wing or an identical image by a plus sign and to represent an inverted image of the wing by a negative sign. This representation gives a clear picture of the system of images required in any problem.

The image system for a small wing midway between two rigid vertical walls at a distance b apart is shown in Fig. 6. The images are identical with the wing itself and comprise two infinite series extending to the right and to the left respectively. The distance of any image from the wing is mb , where m may have any integral value. The induced velocity at the wing due to one of the images is

$$v = \frac{\mu}{4\pi m^2 b^2}$$

and hence the total induced velocity, representing the constraint of the tunnel walls, is

$$v = 2 \sum_1^{\infty} \frac{\mu}{4\pi m^2 b^2} = \frac{\pi \mu}{12 b^2}$$

or

$$\frac{v}{V} = \frac{\pi}{12} \frac{S}{b^2} k_L = 0.262 \frac{S}{b^2} k_L \dots \dots (8.2)$$

If there were only one wall at a distance $\frac{1}{2}b$ from the centre of the wing, the interference would be simply

$$v = \frac{\mu}{4\pi b^2}$$

or

$$\frac{v}{V} = \frac{1}{4\pi} \frac{S}{b^2} k_L = 0.080 \frac{S}{b^2} k_L \dots \dots (8.3)$$

Thus the interference caused by the two walls is 3.29 times that caused by a single wall.

If the rigid walls are replaced by free boundaries, the image system remains the same as in Fig. 6, except that alternate images are of opposite sign. The interference velocity then becomes

$$v = 2 \sum_1^{\infty} (-1)^n \frac{\mu}{4\pi m^2 b^2} = -\frac{\pi}{24} \frac{\mu}{b^2}$$

or

$$\frac{v}{V} = -\frac{\pi}{24} \frac{S}{b^2} k_L = -0.131 \frac{S}{b^2} k_L \quad \dots \quad (8.4)$$

whilst that due to a single free boundary is simply

$$\frac{v}{V} = -\frac{1}{4\pi} \frac{S}{b^2} k_L = -0.080 \frac{S}{b^2} k_L \quad \dots \quad (8.5)$$

and the interference caused by the two free boundaries is only 1.65 times that caused by a single free boundary.

The problem of horizontal boundaries above and below the wing, at a distance h apart can be treated in a similar manner. The images are of alternate sign for rigid boundaries and the interference experienced by the wing is

$$\frac{v}{V} = \frac{\pi}{24} \frac{S}{h^2} k_L = 0.131 \frac{S}{h^2} k_L \quad \dots \quad (8.6)$$

whilst a single horizontal wall gives

$$\frac{v}{V} = \frac{1}{4\pi} \frac{S}{h^2} k_L = 0.080 \frac{S}{h^2} k_L \quad \dots \quad (8.7)$$

When the rigid walls are replaced by free boundaries the images are all identical with the wing. The interference velocity due to two boundaries is

$$\frac{v}{V} = -\frac{\pi}{12} \frac{S}{h^2} k_L = -0.262 \frac{S}{h^2} k_L \quad \dots \quad (8.8)$$

and a single free boundary gives

$$\frac{v}{V} = -\frac{1}{4\pi} \frac{S}{h^2} k_L = -0.080 \frac{S}{h^2} k_L \quad \dots \quad (8.9)$$

Several interesting conclusions can be drawn from an examination of these formulae. Firstly, an aeroplane flying above the ground experiences, according to equation (8.7), an upward induced velocity which reduces the drag at a given value of the lift, and a similar favourable interference is experienced by two aeroplanes flying side by side. Another point to notice is that a change from rigid to free boundaries does not simply change the sign of the interference, but, in accordance with the general theorem established in Section 5,

the interference of rigid vertical walls is of the same magnitude as that of free horizontal boundaries, as may be seen from the pairs of equations (8.2) and (8.8), or (8.4) and (8.6). The analysis also suggests that vertical rigid walls or horizontal free boundaries produce the greatest interference, but the interference of a rectangular tunnel cannot be derived in any simple manner by adding the effects of the vertical and horizontal boundaries. Indeed the results for the vertical and horizontal boundaries themselves show that the interference due to two boundaries bears no simple relationship to that due to a single wall.

9. *Rectangular tunnels.*—The interference experienced by a small wing in a closed rectangular tunnel was calculated by the present author^{2,3} and the analysis for a wing of finite span with uniform or with elliptic distribution of lift has been developed by Terazawa⁸ and Rosenhead¹¹. Other types of rectangular tunnel, with some sides rigid and other sides free, have been considered by Theodorsen¹² and Rosenhead²⁰, the analysis being limited to the problem of small wings. It will be convenient here to discuss first the problem of a small wing in any type of rectangular tunnel, and then to consider the modifications necessary to allow for the finite span of the wing.

The system of images required to represent the constraint of a closed rectangular tunnel of height h and breadth b is shown in Fig. 7. The array comprises alternate rows of positive and negative images, and this system satisfies the necessary condition of zero normal velocity on all the rectangular boundaries. This representation is valid for a wing of finite span with any symmetrical lift distribution, but in the analysis of the problem of small wings each image is assumed to be simply a doublet of strength

$$\mu = VS k_L$$

in accordance with the equation (3.5). The induced velocity at the wing, due to a positive image at the point (mb, nb) , is

$$v = \frac{\mu}{4\pi} \frac{m^2 b^2 - n^2 h^2}{(m^2 b^2 + n^2 h^2)^2}$$

and hence the total induced velocity experienced by the wing is

$$v = \frac{VS k_L}{4\pi} \sum_{-\infty}^{\infty} \sum_{-\infty}^{\infty} (-1)^n \frac{m^2 b^2 - n^2 h^2}{(m^2 b^2 + n^2 h^2)^2}$$

Also the interference factor δ is defined by the equation

$$\frac{v}{V} = \delta \frac{S}{C} k_L \quad \dots \quad (9.01)$$

where C is the tunnel area hb , and the expression for δ in a closed rectangular tunnel is therefore

$$\delta_1 = \frac{hb}{4\pi} \sum_{-\infty}^{\infty} \sum_{-\infty}^{\infty} (-)^n \frac{m^2 b^2 - n^2 h^2}{(m^2 b^2 + n^2 h^2)^2}$$

The summation extends over all positive and negative integral values of m and n excluding the pair (0,0). The evaluation of this double summation³ leads to the expression

$$\delta_1 = 2\pi\lambda \left\{ \frac{1}{24} + \sum_1^{\infty} \frac{pq^{2p}}{1+q^{2p}} \right\} \dots \dots \dots (9.02)$$

where

$$\lambda = \frac{h}{b}$$

$$q = e^{-\pi\lambda}$$

This expression is suitable for numerical calculation, except when λ is very small, since q is very small and only the first few terms of the series need be retained. The validity of the expression has been confirmed by Rosenhead¹¹, who derived it as the limiting form of his solution for a wing of finite span. An alternative form, suitable for small values of λ , can be derived in a similar manner and is

$$\delta_1 = \frac{\pi}{\lambda} \left\{ \frac{1}{24} + \sum_1^{\infty} \frac{(2p-1)r^{2p-1}}{1-r^{2p-1}} \right\} \dots \dots (9.03)$$

where

$$r = e^{-\pi/\lambda}$$

The discussion of the numerical results derived from these formulae will be postponed until the analysis has been developed for some other types of rectangular tunnel.

The results for a closed rectangular tunnel are of great practical importance owing to the existence of many tunnels of this type, but some other types are of interest and illustrate the effect of different boundary conditions. Theodorsen¹² has considered the following five types of rectangular tunnel:

- (1) closed tunnel,
- (2) free jet,
- (3) rigid floor and roof, free sides,
- (4) rigid sides, free floor and roof,
- (5) rigid floor, other boundaries free.

The systems of images corresponding to these different boundary conditions are shown in Figs. 7 and 8, and call for no special comment. They agree with Theodorsen's diagrams except for type (5), where his system is in error* and fails to satisfy the necessary boundary conditions.

* This error has been corrected in the version of Theodorsen's report published in the N.A.C.A. annual volume (1932).

Direct evaluation of the interference factors for these different types of tunnel is unnecessary, since it is possible to establish several interesting relationships between the different types of tunnel and to express all the interference factors in terms of the values of any one type. This analysis depends on the application of the general theorem established in Section 5, which states that the interference experienced by a small wing at the centre of a closed rectangular tunnel of height h and breadth b is of the same magnitude but opposite sign as that on the same wing in a free rectangular jet of height b and breadth h . From this general theorem it follows at once that

$$\delta_2(\lambda) = -\delta_1\left(\frac{1}{\lambda}\right) \dots \dots \dots (9.04)$$

The general theorem also remains valid if the boundary is partly free and partly rigid, and hence

$$\delta_3(\lambda) = -\delta_3\left(\frac{1}{\lambda}\right) \dots \dots \dots (9.05)$$

and

$$\delta_4(\lambda) = -\delta_4\left(\frac{1}{\lambda}\right) \dots \dots \dots (9.06)$$

In particular

$$\delta_2(1) = \delta_4(1) = 0$$

and thus the interference on a small wing in a square tunnel of type (3) or of type (4) is zero.

Some further general relationships can be established by superimposing two of the image systems. We consider simply the doubly infinite array of doublets and ignore the boundary conditions after combining any two systems. By combining types (1) and (3) we obtain a new system of type (1) of double strength and double breadth. Hence

$$v_1(h,b) + v_3(h,b) = 2v_1(h,2b)$$

and remembering, from equation (9.01), that δ is proportional to the product of the velocity v and the tunnel area C , we obtain

$$\delta_1(\lambda) + \delta_3(\lambda) = \delta_1\left(\frac{1}{2}\lambda\right) \dots \dots \dots (9.07)$$

This equation serves to determine the values of δ_3 in terms of the known values of δ_1 .

Similarly by combining the systems (1) and (4) we obtain a new system of type (4) of double strength and double height, and hence

$$\delta_1(\lambda) + \delta_4(\lambda) = \delta_4(2\lambda) \dots \dots \dots (9.08)$$

which connects the values of δ_1 and δ_2 . Another interesting result can be deduced from this last equation in conjunction with the previous equation (9.06). We have

$$\begin{aligned} \delta_1(\lambda) &= \delta_2(2\lambda) - \delta_4(\lambda) \\ &= \delta_4\left(\frac{1}{\lambda}\right) - \delta_4\left(\frac{1}{2\lambda}\right) \\ &= \delta_1\left(\frac{1}{2\lambda}\right) \end{aligned}$$

and hence

$$\left. \begin{aligned} \delta_1(\lambda_1) &= \delta_1(\lambda_2) \\ \text{if } \lambda_1 \lambda_2 &= \frac{1}{2} \end{aligned} \right\} \dots \dots \dots (9.09)$$

This result is a useful check on the numerical values of δ_1 and implies also that the minimum value of δ_1 occurs when $b = \sqrt{2}h$. This minimum value of δ_1 is 0.238.

Finally as regards the tunnel of type (5), we note that the effect of a pair of rows ($\pm n$), cancels out exactly if n is odd. There remain only the even rows which form a system of type (3) of double height, and hence

$$\delta_5(\lambda) = \frac{1}{2} \delta_3(2\lambda) \dots \dots \dots (9.10)$$

By means of these equations it is possible to derive values of all the interference factors from the known values of δ_1 , or more conveniently from those of δ_2 owing to the form of equation (9.08). The interference factor in each type of tunnel can be expressed formally by the double summation

$$\delta = \frac{hb}{4\pi} \sum_{-\infty}^{\infty} \sum_{-\infty}^{\infty} j \frac{m^2 b^2 - n^2 h^2}{(m^2 b^2 + n^2 h^2)^2} \dots \dots (9.11)$$

where j is ± 1 according as the particular image is positive or negative. In particular

$$\begin{aligned} j_1 &= (-1)^n \\ j_2 &= (-1)^m \\ j_3 &= (-1)^{m+n} \\ j_4 &= 1 \end{aligned}$$

but there is no simple expression for j_5 . Direct summation of the expression (9.11) for tunnels of types (2) and (3), by the method used in the original investigation³ of type (1), presents no difficulties, but the application of the same method to the tunnel of type (4) leads to anomalous results since different values are obtained according as the summation is made first with respect to m or with

respect to n . This failure of the method of direct summation is due to inadequate convergence of the series and Theodorsen's results¹² for type (4), obtained by this method, are incorrect.

Rosenhead²⁰ has examined the problem of these five types of tunnel by writing down the appropriate complex potential functions for a wing of finite span and uniform loading in terms of elliptic functions and by proceeding then to the limit of zero span. In particular the resulting expressions for the interference factor in a tunnel of type (4) are

$$\delta_4 = 2\pi\lambda \left\{ \frac{1}{24} - \sum_1^{\infty} \frac{p q^{2p}}{1 - q^{2p}} \right\} - \frac{1}{4} \dots \dots (9.12)$$

and

$$\delta_4 = -\frac{2\pi}{\lambda} \left\{ \frac{1}{24} - \sum_1^{\infty} \frac{p r^{2p}}{1 - r^{2p}} \right\} + \frac{1}{4} \dots \dots (9.13)$$

where

$$\begin{aligned} q &= e^{-\pi\lambda} \\ r &= e^{-\pi/\lambda} \end{aligned}$$

Rosenhead's results are consistent with the various relationships, established previously, connecting the interference factors in the five different types of tunnel. Numerical values of the interference factors are given in Table 3 and the corresponding curves,

TABLE 3

Values of δ in rectangular tunnels

b/h	b/h	δ_1	δ_2	δ_3	δ_4	δ_5
4	1/4	1.047	-0.524	-0.524	0.797	-0.524
2	1/2	0.524	-0.274	-0.250	0.274	-0.282
4/3	3/4	0.351	-0.239	-0.112	0.096	-0.187
1	1	0.274	-0.274	0	0	-0.125
2/3	3/2	0.239	-0.393	0.154	-0.143	-0.056
1/2	2	0.274	-0.524	0.250	-0.274	0
1/4	4	0.524	-1.047	0.524	-0.797	0.125

plotted against the ratio of breadth to height of the tunnel, are shown in Fig. 9. The important practical range is from a square tunnel to a duplex tunnel whose breadth is double the height. In this range the interference in a free jet is numerically greater than that in a closed tunnel, and the interference can be further reduced by using one of the types of tunnel with some free and some rigid boundaries. This conclusion must, however, be accepted with caution since it has been established for small wings only and may require modification when due allowance is made for the finite span of the wing.

The detailed analysis for a wing of finite span has been developed as yet only for a closed rectangular tunnel. Terazawa⁹ first obtained the solution for a wing with uniform distribution of lift across its span. Rosenhead¹¹ repeated this analysis, obtaining his results in a very different mathematical form, and also developed the corresponding analysis for a wing with elliptic distribution of lift across the span. Neither author gives detailed numerical results and their formulae are very inconvenient for numerical computation, but they have been reduced to more suitable forms by the present author¹⁴ and numerical results have been derived for square and duplex tunnels. The general formulae are quoted below, but for the detailed analysis in terms of elliptic functions the reader is referred to Rosenhead's paper.

Writing

$$\sigma = \frac{2s}{b}$$

$$\lambda = \frac{h}{b}$$

$$q = e^{-\pi\lambda}$$

where s is the semi-span of the wing, the value of δ deduced from the assumption of uniform loading is

$$\delta(U) = \frac{\lambda}{2\pi\sigma^2} \log \frac{\pi\sigma}{\sin \pi\sigma} + 2\pi\lambda \sum_1^{\infty} \frac{pq^{2p}}{1+q^{2p}} \left(\frac{\sin \pi p\sigma}{\pi p\sigma} \right)^2 \quad (9.14)$$

and it can easily be verified that the expression tends to the previous form (9.02) as σ tends to zero. The formula deduced from the more reliable assumption of elliptic distribution of lift across the span of the wing is of the more complex form

$$\delta(E) = \lambda F(\sigma) + 8\pi\lambda \sum_1^{\infty} \frac{pq^{2p}}{1+q^{2p}} \left\{ \frac{J_1(\pi p\sigma)}{\pi p\sigma} \right\}^2 \dots \quad (9.15)$$

where J_1 is the Bessel function of the first order and $F(\sigma)$ is a complex power series in σ whose numerical values are given in Table 4. In order to assist any further calculations, values of

TABLE 4
Values of $F(\sigma)$

σ	$F(\sigma)$	σ	$F(\sigma)$
0	0.2618	0.5	0.280
0.1	0.2624	0.6	0.290
0.2	0.2645	0.7	0.304
0.3	0.2679	0.8	0.325
0.4	0.2730	0.9	0.358

the factor in the second term involving Bessel functions are given in Table 5. When σ is zero the expression (9.15) reduces to the previous expression (9.02) and hence this more detailed analysis

TABLE 5
Values of $\left\{ \frac{J_1(\pi x)}{\pi x} \right\}^2$

x	$\left\{ \frac{J_1(\pi x)}{\pi x} \right\}^2$	x	$\left\{ \frac{J_1(\pi x)}{\pi x} \right\}^2$
0	0.250	0.6	0.095
0.1	0.244	0.7	0.064
0.2	0.227	0.8	0.038
0.3	0.200	0.9	0.020
0.4	0.167	1.0	0.008
0.5	0.130	1.2	0.000

serves to check the validity of the summation of the doubly infinite series in the earlier analysis for small wings.

Numerical values derived from these formulae for square and duplex tunnels are given in Table 6, and are exhibited graphically in Fig. 10, where the full curves refer to elliptic and the broken curves to uniform loading. The differences between the results derived from the two types of loading is far less than that in a circular tunnel as given in Table 1 of Section 6, and in Fig. 5. Indeed, until the wing span exceeds 60 per cent. of the tunnel width in a square tunnel or 80 per cent. in a duplex tunnel, there is no appreciable difference between the two sets of results. The increase of the

TABLE 6
Values of δ in closed rectangular tunnels

$2s/b$	Square ($b = h$)		Duplex ($b = 2h$)	
	$\delta(U)$	$\delta(E)$	$\delta(U)$	$\delta(E)$
0	0.274	0.274	0.274	0.274
0.2	0.276	0.275	0.254	0.258
0.4	0.284	0.281	0.214	0.225
0.5	0.292	0.286	0.197	0.208
0.6	0.305	0.295	0.185	0.194
0.7	0.326	0.307	0.181	0.185
0.8	0.362	0.327	0.188	0.183
0.9	0.435	0.359	0.219	0.189

interference factor δ with the span of the wing in a square tunnel is similar to that in a circular tunnel, but in the duplex tunnel there is an important decrease, leading to a minimum value of 0.182, which is 33 per cent. below the value for a small wing, when the wing span is 77 per cent. of the breadth of the tunnel. Since the span of a wing usually lies between 40 per cent. and 60 per cent. of the breadth of the tunnel this feature is important, and the application of the interference factor derived from the consideration of a small wing would overestimate the appropriate correction for tunnel constraint. This result shows that the values of δ , deduced from the consideration of small wings, give only a first approximation to the correction required by a wing of finite span, and that conclusions concerning the relative merits of different types of tunnel must be accepted with caution until the effect of finite span has been investigated.

Experimental checks on the theoretical formulae for the interference in rectangular tunnels have been obtained by Cowley and Jones⁵ and by Knight and Harris¹². Cowley and Jones tested a biplane, formed of two identical rectangular wings of aspect ratio 6 and of 3 ft. span, in 4 ft. and 7 ft. closed square tunnels, and found satisfactory agreement between the two sets of results after correction for tunnel interference according to the theoretical formulae for small wings ($\delta = 0.274$). These experimental results have been corrected again using the values of δ corresponding to the actual span of the biplane, i.e. 0.315 in the 4 ft. tunnel and 0.282 in the 7 ft. tunnel. The uncorrected and corrected polar curves are shown in Fig. 11, and it will be seen that the correction for tunnel interference has brought the two discordant observed curves into almost exact agreement. The correction of the angle of incidence is shown in Fig. 12 and is also very satisfactory, though not quite so good as that of the drag coefficient. It is remarkable that the theoretical formulae, which are developed on the basis of small lift forces, should give satisfactory agreement throughout the whole range up to and including the stall of the wing.

Knight and Harris¹⁰ used three wings of aspect ratio 5 with span-breadth ratios of 0.45, 0.60 and 0.75 respectively. The experiments were made in a free rectangular jet of breadth-height ratio $\sqrt{2}$ at a constant value of the Reynolds number, and the observed values were analysed to deduce the appropriate value of δ for each wing. Values of δ , ignoring the negative sign appropriate

TABLE 7
Rectangular jet

Span/breadth	0.45	0.60	0.75
From drag coefficient	0.420	0.412	0.400
From angle of incidence	0.602	0.402	0.444

to a free jet, are given in Table 7. Ignoring the one discordant value, it would appear that the value of δ is slightly greater than 0.40 and that there is no systematic variation with the span of the wing. Now the value of δ for a small wing in this tunnel would be estimated to be 0.369, being the same as that in a closed rectangular tunnel of breadth-height ratio $1/\sqrt{2}$. Moreover, in such a closed tunnel we should expect some rise of the coefficient δ with the span of the wing in the light of results given in Table 6 and Fig. 10. On the whole, therefore, the value of δ deduced from the experiments appears to be in general agreement with the theoretical calculations.

10. *Elliptic tunnels.*—Closed tunnels can be constructed with any shape of cross-section, but if a free jet is used it is advisable to avoid any corners and the cross-section usually has a circular or oval form. The circular tunnel, for which detailed results have already been obtained, is only a particular case of the more general type of elliptic tunnel, and a knowledge of the interference in rectangular and elliptic tunnels will suffice to give a reasonably reliable estimate of the interference in any type of oval tunnel. The interference experienced by a small wing in an elliptic tunnel has been calculated by the present author¹⁵, and the analysis for a wing with uniform loading has been developed by Sanuki and Tani¹⁷ and for a wing with elliptic loading by Rosenhead¹². Before discussing these results, however, it is proposed to establish an important theorem¹⁵ concerning a wing with elliptic loading in an elliptic tunnel whose foci are situated at the wing tips.

In general it is desirable that the interference factor shall be small, in order to avoid unduly large corrections to the observed results, but the magnitude of these corrections inevitably rises with the size of the wing since it is actually proportional to δS . Another important point is the variation of the induced velocity across the span of the wing, which leads to a distortion of the lift distribution. It has been shown in Section 7 that this effect is unimportant in a circular tunnel, but it would nevertheless be a very desirable quality of a wind tunnel if it gave uniform induced velocity across the span of the wing. This criterion, rather than the magnitude of the interference factor δ really defines the optimum shape of a wind tunnel.

Now consider a wing with elliptic distribution of lift across its span. The flow in a transverse section of the distant wake is that due to a straight line, of length equal to the span of the wing, moving downwards with a constant velocity w , and the complex potential function of this flow is

$$\phi + i\psi = iw(z - \sqrt{z^2 - s^2}) \quad \dots \quad (10.01)$$

where s is the semi-span of the wing. Thus

$$u - iv = iw \left\{ 1 - \frac{z}{\sqrt{z^2 - s^2}} \right\}$$

and at any point of the line itself

$$u = \mp \frac{wx}{\sqrt{s^2 - x^2}}$$

$$v = -w$$

where the upper and lower signs of the expression for u correspond to the upper and lower sides of the line.

Consider next the flow represented by the complex potential function

$$\phi + i\psi = i(w - w')z - iw\sqrt{z^2 - s^2} \dots \dots (10.02)$$

This will give the same tangential component of the velocity as before on both sides of the line and hence the same intensity of the trailing vortices represented by the line, but there is now a uniform interference velocity

$$v = w'$$

Thus the complex potential function (10.02) satisfies the condition of giving uniform interference across the span of the wing, and it remains to examine the conditions under which this flow will arise.

Putting

$$z = s \cosh \zeta \dots \dots (10.03)$$

the complex potential function (10.02) becomes

$$\phi + i\psi = i \{ (w - w') \cosh \xi - w \sinh \xi \} s \cos \eta$$

$$- \{ (w - w') \sinh \xi - w \cosh \xi \} s \sin \eta$$

Now the stream function ψ is constant over the boundary of a closed tunnel, and hence the flow represented by the complex potential function (10.02) will occur in the closed elliptic tunnel defined by the equation

$$w \sinh \xi = (w - w') \cosh \xi$$

Similarly the velocity potential ϕ is constant over the boundary of a free jet, and the shape of the jet is defined by the condition

$$w \cosh \xi = (w - w') \sinh \xi$$

In each case the boundary is represented by a definite value of the parameter ξ , and is therefore an ellipse with foci at the tips of the wing. The semi-axes of the ellipse are

$$a = s \cosh \xi$$

$$b = s \sinh \xi$$

Thus in the closed tunnel

$$\frac{w'}{w} = \frac{a - b}{a}$$

and in the free jet

$$\frac{w'}{w} = -\frac{a - b}{b}$$

Finally, since

$$\frac{w}{V} = \frac{Sk_L}{2\pi s^2}$$

the values of the interference factor in the two tunnels are

$$\delta = \frac{b}{2(a + b)} \dots \dots (10.04)$$

for the closed tunnel, and

$$\delta = -\frac{a}{2(a + b)} \dots \dots (10.05)$$

for the free jet. The condition of uniform interference across the span of the wing is satisfied in any elliptic tunnel, with rigid or free boundary, if the wing extends between the foci of the ellipse and if the lift is distributed elliptically across its span. The condition will also be satisfied approximately for a rectangular wing of the same span, and the optimum shape of tunnel for testing a large wing therefore appears to be one which satisfies this confocal property for the largest span of wing to be used. Since the cross-sectional area C of the tunnel is determined by the wind speed required and by the power available for operating the tunnel, the shape of the tunnel is uniquely determined by the two equations

$$\left. \begin{aligned} a^2 - b^2 &= s^2 \\ \pi ab &= C \end{aligned} \right\} \dots \dots (10.06)$$

The tunnel may have a rigid or a free boundary, but the interference is smaller in the closed tunnel. Numerical values of the interference factor are given in Table 8 and are shown as curves in Fig. 13, the negative sign for the free jet being omitted in the figure. Values of s/\sqrt{ab} are included in the table to show the ratio of the span of the wing to the diameter of the circle of the same area as the ellipse.

TABLE 8
Confocal elliptic tunnels

Breadth/height	1.0	1.5	2.0	2.5	3.0
s/\sqrt{ab}	0	0.913	1.225	1.449	1.633
δ (closed tunnel)	0.250	0.200	0.167	0.143	0.125
δ (free jet)	-0.250	-0.300	-0.333	-0.357	-0.375

Turning next to the problem of a small wing at the centre of any elliptic tunnel, it has been shown by the present author¹⁵ that the problem can be reduced to one of a doubly infinite array of doublets, such as occurs in the problem of rectangular tunnels, by means of the transformation

$$z = c \sin \zeta \dots \dots \dots (10.07)$$

The boundary of the ellipse is taken to be $\eta = 0$ and the semi-axes are then

$$a = c \cosh \theta$$

$$b = c \sinh \theta$$

It is necessary to consider in turn the conditions when the span of the wing lies along the major or along the minor axis of the ellipse, but the results for a free jet can be derived directly from those for a closed tunnel by interchanging the axes of the ellipse and by changing the sign of the interference factor. The resulting formulae are as follows. Writing

$$q = e^{-2\theta}$$

$$r = e^{-\pi^2/2\theta}$$

the interference factor, when the span lies along the major axis of a closed elliptic tunnel, is

$$\delta_1 = \sinh \theta \cosh \theta \sum_1^{\infty} \frac{(2p-1)q^{2p-1}}{1+q^{2p-1}}$$

$$= \frac{1}{4} \sinh \theta \cosh \theta \left\{ \frac{\pi^2}{24\theta^2} + \frac{1}{6} - \frac{\pi^2}{\theta^2} \sum_1^{\infty} \frac{(2p-1)r^{2p-1}}{1+r^{2p-1}} \right\} \dots (10.08)$$

where the alternative values are suitable for large and small values of θ respectively. Similarly, when the span lies along the minor axis of a closed elliptic tunnel, there are the two corresponding expressions

$$\delta_2 = \sinh \theta \cosh \theta \sum_1^{\infty} \frac{(2p-1)q^{2p-1}}{1-q^{2p-1}}$$

$$= \frac{1}{4} \sinh \theta \cosh \theta \left\{ \frac{\pi^2}{12\theta^2} - \frac{1}{6} + \frac{\pi^2}{\theta^2} \sum_1^{\infty} \frac{2p r^{2p}}{1+r^{2p}} \right\} \dots (10.09)$$

These expressions are rather complex, but in practice it suffices almost invariably to retain only the first term of the exponential series, and, unless the ellipse approaches very closely to a circle, the formulae appropriate to small values of θ should be used. Numerical values derived from these formulae are given in Table 9 and are shown as curves in Fig. 14, the full curve corresponding to the closed tunnel and the broken curve to the free jet, but without the appropriate negative sign. The interference is least in a broad

closed tunnel or in a narrow free jet, and the minimum value occurs when the major axis is approximately 1.35 times the minor axis. Indeed the results are similar to those already obtained for rectangular tunnels, but the values of the interference factor are slightly lower in an elliptic than in a rectangular tunnel for equal values of the ratio of breadth to height. In general the span of the wing will be along the major axis of the ellipse and the interference is then less in a closed tunnel than in a free jet.

TABLE 9
Closed elliptic tunnels

Breadth/height.. δ	0.305	0.553	0.781	1.000	1.280	1.795	3.280
	0.686	0.388	0.292	0.250	0.231	0.243	0.364

The interference experienced by a wing with uniform distribution of lift across its span has been determined by Sanuki and Tani¹⁷. The span of the wing is assumed to lie along the major axis of the ellipse and the solution is obtained by expressing the stream function of the flow by suitable infinite series. Results are given for closed tunnels and for free jets. The more important solution for a wing with elliptic distribution of lift across its span has been obtained by Rosenhead¹⁹ in terms of elliptic functions. The resulting formulae are very complex, but numerical values of δ have been calculated by Rosenhead for closed tunnels and for free jets, and are reproduced here in Tables 10 and 11. In these tables the span

TABLE 10
Closed elliptic tunnels

Breadth/height.	1/2	2/3	1	3/2	2.
$\frac{z}{c} = 0$	0.427	0.331	0.250	0.231	0.254
0.2	0.438	0.334	0.250	-0.228	0.245
0.4	0.485	0.344	0.250	0.221	0.222
0.6		0.467	0.250	0.212	0.186
0.8		0.427	0.250	0.204	0.176
1.0			0.250	0.200	0.167

of the wing is expressed as a fraction of the distance ($2c$) between the foci of the ellipse. When the breadth of the ellipse exceeds its height, the ratio of the span of the wing to the breadth of the tunnel is

$$\frac{s}{a} = \frac{s}{c} \sqrt{1 - \frac{b^2}{a^2}} \dots \dots (10.10)$$

and when the height of the ellipse exceeds the breadth the corresponding formula is

$$\frac{s}{b} = \frac{s}{c} \sqrt{\frac{a^2}{b^2} - 1} \dots \dots \dots (10.11)$$

where *a* and *b* are the semi-axes of the ellipse. The results for a circular tunnel are not revealed by these tables, since the span of the wing is zero for all values of *s/c*. Full results for the circular tunnel have, however, already been given in Section 6.

Rosehhead's values of δ are also shown in Figs. 15 and 16, where the abscissa is the ratio of the span of the wing to the breadth of

TABLE 11
Free elliptic jets

Breadth/height.	1/2	2/3	1	3/2	2
$\frac{s}{c} = 0$	-0.254	-0.231	-0.250	-0.331	-0.427
0.2	-0.265	-0.234	-0.250	-0.328	-0.416
0.4	-0.311	-0.244	-0.250	-0.321	-0.392
0.6		-0.267	-0.250	-0.312	-0.365
0.8		-0.296	-0.250	-0.304	-0.342
1.0			-0.250	-0.300	-0.333

the tunnel. In a closed tunnel the value of δ increases with the span of the wing when the breadth of the tunnel is less than the height, but decreases in the more usual condition with the span of the wing along the major axis of the ellipse. These results are similar to those obtained previously for rectangular tunnels and shown in Fig. 10. The corresponding values of δ in a free elliptic jet are shown in Fig. 16, and it will be noticed that the numerical value of δ never decreases to the same extent as in the closed tunnels.

No experimental checks on the value of δ in elliptic wind tunnels are available, but Knight and Harris¹⁰ have obtained results in two oval jets with semi-circular ends, the ratios of breadth to height being respectively $\sqrt{2}$ and 2. Sanuki and Tani¹⁷ have made an approximate theoretical calculation of the value of δ to be expected in the first of these two tunnels and the comparison with the values deduced from an analysis of the experimental results is given in Table 12, where the negative sign appropriate to a free jet is ignored. The calculated values, which are based on the assumption of uniform distribution of lift across the span of the wing, are in fair agreement with the values deduced from the drag coefficients, whilst the analysis of the angles of incidence leads to rather higher values as noticed previously for circular tunnels.

TABLE 12
Oval jet

Span/breadth	0.45	0.60	0.75
From angle of incidence	0.498	0.386	0.388
From drag coefficient	0.340	0.320	0.328
Calculated	0.295	0.290	0.300

11. *Downwash and tailsetting.*—Hitherto the analysis has been confined to the problem of the interference experienced by a wing in a wind tunnel, though the experimental work of Cowley and Jones⁵, illustrated in Figs. 11 and 12, indicates that the results of the analysis can also be applied successfully to a biplane system. If, however, the complete model of an aeroplane is tested in a wind tunnel, it is evident that the interference experienced by the tailplane, situated some distance behind the wings, may differ from that experienced by the wings themselves. In other words, there will be an interference on the angle of downwash behind the wings and on the tailsetting required to trim the aeroplane. Let ϵ_1 be the induced angle of upwash experienced by the wings, and let ϵ_2 be the additional angle of upwash in the neighbourhood of the tailplane of a model aeroplane. As a consequence of this interference the downwash angle ϵ and the tailsetting η_T to trim the aeroplane at a given value of the lift coefficient will be measured smaller in a wind tunnel than in free air and will require the corrections

$$\left. \begin{aligned} \Delta\epsilon &= \epsilon_1 + \epsilon_2 \\ \Delta\eta_T &= \epsilon_2 \end{aligned} \right\} \dots \dots \dots (11.1)$$

The lift of the aeroplane may be assumed to be given wholly by the wings, and thus ϵ_1 can be expressed in the form

$$\epsilon_1 = \delta \frac{S}{C} k_L \dots \dots \dots (11.2)$$

where δ is the interference factor whose value, in different types of wind tunnel, has been considered in the previous sections. It is now necessary to determine the additional interference ϵ_2 in the neighbourhood of the tailplane of an aeroplane.

The problem of this additional interference in a closed rectangular wind tunnel has been considered by Glauert and Hartshorn⁶ who have obtained the solution on the assumption that the distance of the tailplane behind the wing is of the same order of magnitude as the semi-span of the wing, and that the dimensions of the wing itself are small compared with those of the tunnel. The solution therefore corresponds to the conditions assumed for small wings in the earlier analysis.

The systems of images used to represent the constraint of the boundaries of a rectangular tunnel have previously been considered only in relationship to the two-dimensional problem of a transverse section of the wake behind a wing, but it can easily be seen that this method of images is equally valid for the three-dimensional problem of the whole tunnel. Thus, for example, if two identical aeroplanes are flying side by side, there will be no flow across the vertical plane midway between them and this plane can be replaced by a rigid boundary without modifying the flow in any way. In fact all the systems of images, used in the discussion of different types of rectangular tunnels, remain valid for the three-dimensional problem, but a positive image must now be interpreted as a system identical with the wing itself, including both the circulation round the wing and the accompanying system of trailing vortices.

By considering each image in turn it is possible to write down an expression, involving doubly infinite summation, for the induced velocity at any point of the tunnel. The analysis is simplified if the span of the wing is small compared with the dimensions of the tunnel, and if the induced velocity is calculated only at a point of the central axis of the tunnel at a small distance l behind the wing. The expression for the excess of the induced angle of upwash at this point over the value at the wing itself, is then

$$e_2 = \frac{15 k_L}{4\pi} \sum_{-\infty}^{\infty} \sum_{-\infty}^{\infty} (-1)^n \frac{m^2 b^2 - 2n^2 h^2}{(m^2 b^2 + n^2 h^2)^{5/2}} \quad \dots \quad (11.3)$$

No simple expression for this doubly infinite sum can be obtained and it is necessary to evaluate the sum numerically for each shape of tunnel. The results are expressed conveniently in the form

$$e_2 = \delta' \frac{15}{hC} k_L \quad \dots \quad (11.4)$$

and numerical values for the two most important types of closed rectangular tunnel are given in Table 13. The expression for e_2 in a free rectangular jet is identical with (11.3) except that the factor $(-1)^n$ is changed to $(-1)^{2n}$. Unfortunately, however, there is no simple connection between the results in closed tunnels and free jets, such as occurs in the case of the interference experienced by the wing itself, but the numerical value of δ' for a free square jet is included in the table. It will be noticed that this value is numerically smaller than that in a closed square tunnel. These values refer only to small wings and may need modification when due allowance is made for the actual span of the wings. The value of δ , which defines the interference on the wing itself, varies with the span of the wing in a closed tunnel as shown in Fig. 10, and there will probably be a sympathetic variation of the value of δ' . Values of the ratio of δ' to δ have therefore been included in Table 13 and, failing more definite information, these values may be used to determine the appropriate value of δ' , in any particular problem.

TABLE 13
Rectangular tunnels

Type.	b/h	δ'	δ'/δ
Closed tunnel	1.0	0.480	1.75
Closed tunnel	2.0	0.585	2.13
Free jet	1.0	-0.407	1.48

An attempt to derive a formula for the interference on the angle of downwash in a circular tunnel has been made by Seiferth¹⁸ but unfortunately there is no simple image system which represents accurately the conditions of this three-dimensional problem. The vortex images of the two-dimensional problem of a transverse section of the wake can be extended forwards parallel to the trailing vortices of the wing as far as the transverse plane through the wing itself, but it is not possible to complete the image system in any simple manner by transverse vortices which will satisfy the necessary boundary conditions. Seiferth's formula represents merely the effect of these longitudinal image vortices and is therefore incorrect in principle. Moreover his expression is of the form

$$e_2 = \delta' \frac{15S}{a^2 C} k_L$$

where a is the radius of the tunnel and s is the semi-span of the wing. This formula contains the fourth power of the linear dimensions of the tunnel in the denominator, whereas the previous formula (11.4) for a rectangular tunnel contains only the third power of these dimensions. Thus Seiferth's formula appears also to be incorrect in form. Indeed we may anticipate that the interference in a circular tunnel will not differ greatly from that in a square tunnel of corresponding size. The interference on the wing itself is

$$e_1 = 0.250 \frac{S}{C} k_L$$

in a circular tunnel, and

$$e_1 = 0.274 \frac{S}{C} k_L$$

in a square tunnel. These expressions give equal values if the side of the square is 0.925 times the diameter of the circle. If we assume that the interference on the angle of downwash will also have equal values in the two tunnels, the formula for this interference in a circular tunnel becomes

$$e_2 = \delta' \frac{15}{aC} k_L \quad \dots \quad (11.5)$$

where d is the diameter of the tunnel, and the numerical value of δ' does not differ by more than 1 per cent. from that appropriate to a square tunnel. In the absence of a true solution of the problem in a circular tunnel, it is suggested therefore that the interference on the angle of downwash and tailsetting may be estimated approximately from the formula (11.5) using the same value of δ' as in a square tunnel.

Experimental confirmation of the accuracy of the formulae for the interference on the angle of downwash and tailsetting in a closed square tunnel has been obtained by Glauert and Hartshorn* by testing a complete model aeroplane in a 4 ft. and in a 7 ft. tunnel. The uncorrected and the corrected results are shown in Figs. 17 and 18, and it will be seen that the application of the theoretical corrections for tunnel interference has brought the discordant observed results of the two tunnels into excellent agreement.

12. *Maximum lift coefficient.*—The preceding analysis of the interference experienced by a wing in any type of wind tunnel has been developed on the basis and principles of modern aerofoil theory, which is essentially an approximate theory suitable for small lift forces. The experimental results, which have been obtained as checks on the theoretical formulae, have however shown that the analysis remains valid over a wider range than might have been anticipated and that in fact it may be applied with confidence throughout the usual working range of a wing. On the other hand the analysis gives no direct indication whether there is a tunnel constraint of the maximum lift coefficient of a wing, and it is in fact incapable of giving an exact answer to this question, though it is possible to deduce some conclusions regarding the general nature of this interference.

Consider first an untwisted wing of elliptic plan form in an infinite fluid. The downward induced velocity, due to the system of trailing vortices, has a constant value across the span of the wing, and each section of the wing operates at the same effective angle of incidence. Hence we may anticipate that every section will reach its critical angle simultaneously and that the maximum lift coefficient of the elliptic wing will be sensibly the same as that of the aerofoil section in two-dimensional motion. Considering next a wing of rectangular plan form, the downward induced velocity is least at the centre of the wing and increases outwards towards the tips. Thus the centre of the wing stalls first and the maximum lift coefficient of the rectangular wing will tend to be lower than that of an elliptic wing of the same aerofoil section. Now in a closed wind tunnel a wing experiences an upward induced velocity, due to the constraint of the tunnel walls, which is least at the centre of the wing and increases outwards towards the tips. This interference will therefore tend to counteract in part the ordinary induced velocity of a rectangular wing, and we may anticipate a corresponding

increase in the value of the maximum lift coefficient. Similarly there will tend to be a decrease of the maximum lift coefficient in a free jet. The tunnel constraint on the distribution of lift across the span of a wing is, however, known to be small unless the span of the wing is a large fraction of the breadth of the tunnel, and we may, therefore, anticipate only a small interference on the maximum lift coefficient of a wing, depending mainly on the breadth of the tunnel.

Another type of interference on the maximum lift coefficient may occur if the chord of the wing is large. Consider, for simplicity, a single horizontal boundary above the wing. The wing and its image will then form a divergent passage, which will tend to cause a breakdown of the flow over the upper surface of the wing and hence a reduction of the value of the maximum lift coefficient. This second type of interference will depend mainly on the ratio of the chord of the wing to the height of the tunnel.

It is not possible to estimate the magnitude of these interference effects, since they depend on the stability of the flow over the upper surface of the wing near the critical angle of incidence. It is necessary to turn to experimental results, but here again it is difficult to obtain a reliable answer owing to the variation of the maximum lift coefficient of a wing with the scale of the test and with the turbulence of the wind stream. Results obtained in different wind tunnels or at different values of the Reynolds number are, therefore, of little value in this connection, but there are available a few series of experimental results from which it is possible to deduce some tentative empirical conclusions.

A detailed investigation of the tunnel interference on the maximum lift coefficient of rectangular wings has been made by Bradfield, Clark and Fairthorne*. The main series of experiments was made in a closed 7 ft. wind tunnel, inside which smaller tunnels were constructed by the use of false floors and sides. Thus it was possible to test a wing in tunnels of different size and shape whilst maintaining the same value of the Reynolds number and the same

TABLE 14

Maximum lift coefficient in closed tunnels

Tunnel.		R.A.F. 30	Aerofoil A	R.A.F. 32	R.A.F. 19
b	h	(8 × 48 in.)	(6 × 36 in.)	(8 × 48 in.)	(5½ × 33 in.)
7	7	0.415	0.511	0.653	0.898
7	3½			0.660	0.912
4½	7			0.678	0.928
4½	4½	0.443	0.528	0.682	0.926
3½	7				0.934
3½	3½		0.545		0.938

degree of turbulence of the wind stream. The experimental results for four rectangular wings of aspect ratio 6 are summarised in Table 14, each value being the mean of the results obtained at wind speeds of 60 and 80 ft./sec. It will be noticed that the value of the maximum lift coefficient increases as the size of the tunnel decreases, and that the effect is due mainly to the breadth of the tunnel whilst changes of the height of the tunnel produce only small effects in general. In Fig. 19 the values of the maximum lift coefficient have been plotted against the ratio (S/b^2) of the area of the wing to the square of the breadth of the tunnel. The points for each wing lie on a set of straight lines of approximately the same slope and to a close approximation it is possible to write for all wings which give widely different values of the maximum lift coefficient,

$$\Delta k_L (\text{max}) = 0.38 \frac{S}{b^2} \quad \dots \quad (12.1)$$

The maximum error due to the use of this simple formula appears to be of the order of ± 0.005 in the value of the maximum lift coefficient.

The same authors⁹ quote results for a group of slotted wings tested in a 4 ft. and in a 7 ft. tunnel. A check test on one of the wings in a small tunnel, constructed inside the 7 ft. tunnel, suggested that there was no important difference in the effective turbulence of the two tunnels, and the results may therefore be accepted as giving a fair measure of the tunnel interference. These results are collected in Table 15 and it appears that the mean increment of the maximum lift coefficient is 0.12, whereas the empirical formula (12.1) would have suggested a value of 0.024 only. Thus there appears to be an increased tunnel interference on the maximum lift coefficient of a slotted wing, but there are unfortunately no results available for a more detailed analysis of this rather peculiar result.

The four wings of Table 14 have also been tested in a 5 ft. free jet⁹ but the results cannot be accepted as reliable determinations of the tunnel interference owing to possible differences of the turbulence of the stream. The aerofoil section A is however

TABLE 15
Maximum lift coefficient of slotted wings in closed tunnels

Slotted Wing.	4 ft. tunnel.	7 ft. tunnel.
R.A.F.6	0.94	0.80
Aircrow 3	1.08	0.92
Aircrow 4	1.02	0.95
R.A.F. 28	0.87	0.75
R.A.F.28 (larger slot)	0.985	0.865

known to be insensitive to changes of Reynolds number, and hence is also probably insensitive to changes of turbulence, and the values of the maximum lift coefficient of this wing are as follows:—

5 ft. free jet ..	0.492
Free air	0.500

The free air value was estimated from the tests in the series of closed tunnels, and there appears to be a small decrease of the maximum lift coefficient in the free jet. Some other experimental results, obtained by Prandtl⁴ by testing a series of rectangular wings of aspect ratio 5 and of section Göttingen 389, are given in Table 16. These results show very little change of the maximum lift coefficient. There is a slight increase with the size of the wing, but the larger wings were tested at lower wind speeds in order to maintain a constant value of the Reynolds number, and this change of wind speed may have been accompanied by a change of turbulence.

TABLE 16

Maximum lift coefficient in a free jet

S/C	0.018	0.040	0.072	0.112	0.162
k_L (max.) ..	0.560	0.553	0.567	0.569	0.570

The evidence regarding the maximum lift coefficient of a wing in a free jet is inconclusive, but the interference undoubtedly is very small and may be neglected except for unusually large wings.

PART 2

Wings, Two Dimensions

13. *Induced curvature of the flow.*—The preceding discussion and analysis have been devoted to the problem of a wing of finite span in a wind tunnel, and it is now necessary to consider the nature of the interference when the wing stretches across the whole breadth of the tunnel. If, for example, a wing stretches from wall to wall of a closed rectangular tunnel there will be no system of trailing vortices, apart from any minor effects due to the boundary layer along the wall of the tunnel, and the preceding method of analysis would suggest that the wing experiences no interference. There is, however, a constraint of the flow imposed by the roof and floor of the tunnel, and it is necessary to develop a method of estimating the magnitude of this constraint. The failure of the preceding analysis to give any indication of this interference is due to the underlying assumption that a wing may be replaced by a lifting

line or bound vortex along its span. Consequently the formulae for the interference are really independent of the chord of the wing and the appearance of the wing area S in a formula of the type

$$\Delta\alpha = \delta \frac{S}{c} k_L$$

is due solely to the definition of the lift coefficient. The formulae for the corrections to the angle of incidence and drag may be written in the alternative forms

$$\Delta\alpha = \delta \frac{L}{C_D V^2}$$

and

$$\Delta D = \delta \frac{L^2}{C_D V^2}$$

where δ depends on the shape and nature of the wind tunnel, on the ratio of the span of the wing to the breadth of the tunnel, and on the distribution of lift across the span of the wing. It is evident that these formulae are quite independent of the chord and area of the wing, and their validity has been fully justified by the experimental results available. This result is due to the fact that the chord of a wing of finite span will in general be only a small fraction of the height of the tunnel, but, when we turn to the problem of a wing stretching across the whole breadth of the tunnel, the chord of the wing will tend to be larger and, in order to obtain reliable estimates of the interference experienced by the wing, it is necessary to consider the finite extension of the chord.

The problem to be considered is one of flow in two dimensions only, since the flow may be assumed to be the same in all planes normal to the span of the wing. Exact solutions of the problem have been obtained for thin symmetrical aerofoil sections, but it is more instructive to consider in the first place an approximate method of solution which reveals more clearly the nature of the interference due to the tunnel. Consider a closed tunnel of height h with parallel rigid boundaries above and below the wing. The boundary conditions are satisfied exactly by the introduction of an infinite column of images above and below the wing, the images being alternately inverted and direct replicas of the wing itself. Similarly the conditions in a free jet may be represented by an infinite column of images identical with the wing.

In order to appreciate the nature of the interference due to these images it is convenient to consider the effect of a single direct image as illustrated in Fig. 20. Consider first the effect of a point vortex of strength K at the point C . The induced velocity at a point O at height h above C is wholly horizontal and of magnitude

$$u = \frac{K}{2\pi h}$$

The effect of a pair of similar images at equal distances above and below the point O will cancel out exactly and there is no resultant induced velocity due to the series of images appropriate to a closed tunnel or to a free jet. We note, however, that the induced flow at O due to the point vortex at C is curved; there is an upward induced velocity in front of O and a downward induced velocity behind O , and this curvature of the induced flow is in the same sense whether the inducing vortex is above or below the wing. Thus the wing at O is situated in a curved flow, and this curvature of the flow will modify the force experienced by the wing. Thus a symmetrical wing at zero angle of incidence would give zero lift in an unlimited stream, but in order to obtain zero lift in the induced curved flow it would be necessary to increase the camber of the wing in accordance with the curvature of the flow. Actually the lift of a given wing will be reduced by an amount corresponding to an effective reduction of camber of this magnitude. It is convenient in the first place to calculate this curvature correction due to a single direct image of the wing, which is in effect the problem of biplane wings of infinite span as considered by the present author²². The correction in a closed tunnel or free jet can then be derived by a simple process of summation over all the images.

Referring to Fig. 20, if w is the downward induced velocity at a point P of the wing at a distance x behind O , the radius of curvature R of the streamlines is given by the equation

$$\frac{V}{R} = \frac{dw}{dx}$$

and the relationship between the camber and radius of a circular arc is

$$\gamma = \frac{c}{8R}$$

Thus the effective reduction of camber of the wing due to the induced flow is

$$\gamma = \frac{c}{8V} \frac{dw}{dx} \dots \dots \dots (13.01)$$

Also the induced velocity at the point P is

$$w = \frac{K}{2\pi} \frac{x}{h^2 + x^2} \dots \dots \dots (13.02)$$

and hence

$$\frac{dw}{dx} = \frac{K}{2\pi} \frac{h^2 - x^2}{(h^2 + x^2)^2} \dots \dots \dots (13.03)$$

As a first approximation we may assume the chord of the wing to be very small and may represent the wing by a concentrated point vortex of strength K , where

$$K = k_L cV \quad \dots \quad (13.04)$$

On this basis we put $x = 0$ in the equations for the induced velocity and camber. The induced velocity is zero, but there is an effective reduction of camber of magnitude

$$\gamma = \frac{1}{16\pi} \left(\frac{c}{h}\right)^2 k_L \quad \dots \quad (13.05)$$

In a free jet we shall obtain

$$\gamma = \frac{1}{8\pi} \left(\frac{c}{h}\right)^2 k_L \sum_1^{\infty} \frac{1}{n^2} = \frac{\pi}{48} \left(\frac{c}{h}\right)^2 k_L$$

and in a closed channel

$$\gamma = \frac{1}{8\pi} \left(\frac{c}{h}\right)^2 k_L \sum_1^{\infty} \frac{(-1)^n}{n^2} = -\frac{\pi}{96} \left(\frac{c}{h}\right)^2 k_L$$

These results were given by Prandtl¹ in his original paper on wind tunnel interference and have been reproduced by other writers, but the approximation is in fact too crude and is not a true representation of the effective camber to the order $(c/h)^2$. The discrepancy arises from the fact that the correction to the camber must be applied with reference to the mid point of the wing, whereas the point vortex representing the circulation round the wing must be placed at the centre of pressure, which is the centroid of the bound vortices distributed along the chord of the wing.

Proceeding to this closer approximation, let θ be the centre of pressure coefficient of the wing, related to the coefficient of the moment about the leading edge by the equation

$$k_m = -\theta k_L$$

The coordinate of the midpoint of the wing is then

$$x = (0.5 - \theta)c$$

and in accordance with the previous equations (13.02) and (13.04) the normal induced velocity at this point, to the order of accuracy $(c/h)^2$, is

$$\begin{aligned} w &= \frac{V}{2\pi} \left(\frac{c}{h}\right)^2 (0.5 - \theta)k_L \\ &= \frac{V}{4\pi} \left(\frac{c}{h}\right)^2 (k_L + 2k_m) \quad \dots \quad (13.06) \end{aligned}$$

No correction is required to the expression (13.05) for the effective camber to this same order of accuracy, since the retention of x in

equation (13.03) would lead to a term of order $(c/h)^4$. This closer analysis of the problem shows that the total interference due to the curvature of the flow comprises the effective change of camber (13.05) and a change of the effective angle of incidence corresponding to the induced velocity (13.06).

Now the characteristics of a circular arc aerofoil of camber γ are given by the equations

$$k_L = \pi (\alpha + 2\gamma)$$

and

$$k_m = -\frac{1}{4}k_L - \frac{\pi}{2}\gamma$$

Comparing the wing subjected to interference with the same wing in an unlimited stream, the increase of the moment coefficient due to the effective reduction of camber is

$$k_m - k_m(f) = \frac{1}{32} \left(\frac{c}{h}\right)^2 k_L$$

and the slope of the moment curve is

$$\frac{dk_m}{dk_L} = -\frac{1}{4} \left\{ 1 - \frac{1}{8} \left(\frac{c}{h}\right)^2 \right\} \quad \dots \quad (13.07)$$

Similarly the increase of the angle of incidence, necessary to maintain the same value of the lift coefficient, is

$$\begin{aligned} \alpha - \alpha(f) &= \frac{w}{V} + 2\gamma \\ &= \frac{1}{8\pi} \left(\frac{c}{h}\right)^2 (3k_L + 4k_m) \quad \dots \quad (13.08) \end{aligned}$$

or alternatively the decrease of the lift coefficient at the same angle of incidence is

$$k_L(f) - k_L = \frac{1}{8} \left(\frac{c}{h}\right)^2 (3k_L + 4k_m) \quad \dots \quad (13.09)$$

Finally the moment coefficient of an aerofoil in an unlimited stream can be written in the form

$$k_m = \mu - \frac{1}{4}k_L$$

and this relationship can be used as an approximation in the expressions for the corrections to the angle of incidence and lift coefficient, which then become

$$\alpha - \alpha(f) = \frac{1}{4\pi} \left(\frac{c}{h}\right)^2 (k_L - 2\mu) \quad \dots \quad (13.10)$$

and

$$k_L(f) - k_L = \frac{1}{4} \left(\frac{c}{h} \right)^2 (k_L + 2\mu) \quad \dots \quad (13.11)$$

In general μ is small compared with k_L , and it is zero for a symmetrical section. The correction to the angle of incidence or lift coefficient is then double the value which would be deduced by the first approximation due to the effective camber (13.05), ignoring the induced velocity at the centre of the wing (13.06). The formulae (13.07) to (13.11) give the effect of a single image, identical with the wing itself, but the interference due to the infinite columns of images representing a free jet or closed tunnel can be derived quite simply by multiplying the expressions for the interference by an appropriate factor. This factor is $\pi^2/3$ for a free jet and $-\pi^2/6$ for a closed tunnel. In particular the lift at a given angle of incidence is decreased in a free jet and increased in a closed tunnel.

14. *Free jets.*—In the preceding section expressions have been obtained for the interference on the characteristics of a wing in a free jet or closed tunnel due to the induced curvature of the flow in the neighbourhood of the wing. This is the only interference in a closed tunnel, but there is an additional type of interference in a free jet owing to the downward deflection of the jet behind the wing. The magnitude of this additional interference, which is in fact far more important than that due to the curvature of the flow, has been determined by Prandtl by considering the appropriate system of images¹ and alternatively by considering the downward momentum imparted to the jet². The rate of mass flow in a jet of height h and breadth b is $\rho V h b$ and the ultimate downward velocity w_0 imparted to the jet by the lift of the wing is therefore determined by the equation

$$\rho V h b w_0 = \rho V^2 b c k_L$$

or

$$\frac{w_0}{V} = \frac{c}{h} k_L$$

Now the jet approaches the wing horizontally, and the downward induced velocity w experienced by the wing will be half the ultimate downward velocity of the wake. Thus

$$\frac{w}{V} = \frac{1}{2} \frac{c}{h} k_L$$

As a consequence of this downward velocity the angle of incidence of the wing in the jet must be increased, in order to maintain the same value of the lift coefficient as in an unlimited stream, by the amount

$$\alpha - \alpha(f) = \frac{1}{2} \frac{c}{h} k_L \quad \dots \quad (14.1)$$

and the induced drag coefficient of the wing in the jet will be

$$k_D = \frac{1}{2} \frac{c}{h} k_L^2 \quad \dots \quad (14.2)$$

Alternatively, at the same angle of incidence in the jet and in an unlimited stream, we have

$$\begin{aligned} k_L &= \pi \left(\alpha - \alpha_0 - \frac{1}{2} \frac{c}{h} k_L \right) \\ &= k_L(f) - \frac{\pi c}{2 h} k_L \end{aligned}$$

where α_0 is the angle of zero lift of the wing, and thus

$$\frac{L_0}{L} = 1 + \frac{\pi c}{2 h} \quad \dots \quad (14.3)$$

where L_0 is the lift in an unlimited stream and L is the lift in the free jet at the same angle of incidence.

Combining these downwash corrections to the characteristics of a wing in a free jet with the previous results for the effect of the induced curvature of the flow, the final formulae for the characteristics of a wing in a free jet are as follows. At a definite value of the lift coefficient, the necessary increase of the angle of incidence in the jet is

$$\alpha - \alpha(f) = \frac{1}{2} \frac{c}{h} k_L + \frac{\pi}{12} \left(\frac{c}{h} \right)^2 (k_L + 2\mu) \quad \dots \quad (14.4)$$

the increase of the drag coefficient in the jet is

$$k_D - k_D(f) = \frac{1}{2} \frac{c}{h} k_L^2 \quad \dots \quad (14.5)$$

to which it may be necessary to add a small correction owing to the change in the effective camber of the wing, and the expression for the moment coefficient in the jet is

$$k_m = \mu - \frac{1}{4} \left\{ 1 - \frac{\pi^2}{24} \left(\frac{c}{h} \right)^2 \right\} k_L \quad \dots \quad (14.6)$$

Alternatively, if the small correction due to μ in equation (14.4) is neglected, the ratio of the lift of a wing in an unlimited stream to its lift in a free jet at the same angle of incidence is

$$\frac{L_0}{L} = 1 + \frac{\pi c}{2 h} + \frac{\pi^2}{12} \left(\frac{c}{h} \right)^2 \quad \dots \quad (14.7)$$

This equation applies strictly to wings of symmetrical section, but will also be approximately true for all wings except at very small values of the lift coefficient.

These formulae have been derived by an approximate method of analysis suitable for small values of c/h , but an exact solution for a straight line aerofoil, corresponding in practice to a thin symmetrical section, has been obtained by Sasaki²³. The analysis is of a complex form, but Sasaki has given numerical results for a range of values of c/h and for an angle of incidence of 10 deg., corresponding to a lift coefficient of 0.545 in an unlimited stream. These results are reproduced in Table 17. Sasaki's results have been compared with the approximate formula (14.3) by Karman²⁴. This comparison is shown in Fig. 21, together with the curve of the second approximation (14.7) which includes the effect of the induced curvature of the

TABLE 17
Free jet ($\alpha = 10^\circ$)

c/h	L/L_0	D/L	$2k_D/k_L^2$
0	1	0	0
0.051	0.924	0.0128	0.051
0.128	0.826	0.0287	0.128
0.260	0.680	0.0483	0.261
0.425	0.532	0.0619	0.427

flow. The agreement of this second approximation with Sasaki's accurate results is very good for moderate values of c/h . Also the figure shows clearly that the interference is due mainly to the downward deflection of the jet behind the wing, but that the effect of the induced curvature of the flow is quite appreciable. The last column of Table 17 has been added to Sasaki's table for comparison with the approximate formula (14.5) and it appears that this formula gives an accurate estimate of the increased drag of a wing in a free jet. This comparison with Sasaki's exact analysis of the problem shows that the approximate formulae (14.4) to (14.7) are sufficiently accurate for reasonable values of c/h , and the approximate analysis has shown that the interference is due mainly to the downward deflection of the free jet behind the wing, and partly to the induced curvature of the flow past the wing.

15. *Closed wind tunnels.*—In a closed tunnel, where the flow is constrained by rigid parallel walls above and below the wing, there is no general deflection of the stream behind the wing, such as occurs in a free jet, and the interference experienced by the wing is simply that due to the induced curvature of the flow. The interference is therefore given by the equations of Section 13 with the

addition of the factor $-\pi^2/6$ appropriate to a closed tunnel. At a definite value of the lift coefficient, the decrease of the angle of incidence in the tunnel is

$$\alpha(f) - \alpha = \frac{\pi}{24} \left(\frac{c}{h}\right)^2 (k_L + 2\mu) \dots \dots (15.1)$$

and the expression for the moment coefficient is

$$k_m = \mu - \frac{1}{4} \left\{ 1 + \frac{\pi^2}{48} \left(\frac{c}{h}\right)^2 \right\} \dots \dots (15.2)$$

whilst there is no change of drag. Alternatively, if the small correction due to μ in equation (15.1) is neglected, the ratio of the lift of a wing in an unlimited stream to its lift in the tunnel at the same angle of incidence is

$$\frac{L_0}{L} = 1 - \frac{\pi^2}{24} \left(\frac{c}{h}\right)^2 \dots \dots (15.3)$$

This relationship applies strictly to wings of symmetrical section, but will also be approximately true for all wings except at very small values of the lift coefficient.

Sasaki²³ attempted to obtain an exact solution for a straight line aerofoil but his analysis contains a mathematical error. The correct solution has been obtained by Rosenhead²⁵ and his values of L/L_0 are given in Table 18. For small and moderate values of the lift coefficient a single curve of L/L_0 can be drawn against c/h , but separate curves are obtained for values of the lift coefficient equal to or exceeding 0.5. These curves are shown in Fig. 22 where each curve corresponds to a definite value of the lift coefficient in an unlimited stream. In the ordinary practical range, where c/h does not exceed 0.5 and the lift coefficient itself is not unduly high, it is sufficiently accurate to ignore these minor variations

TABLE 18
Closed tunnel, values of L/L_0

$\frac{c}{h} =$	0.10	0.20	0.30	0.40	0.50	0.70	0.90
$k_L = \text{small}$	1.004	1.016	1.036	1.060	1.094	1.175	1.270
0.50	1.004	1.016	1.037	1.062	1.098	1.185	1.285
0.75	1.004	1.017	1.038	1.065	1.103	1.198	1.307
1.00	1.004	1.017	1.040	1.069	1.109	1.215	1.338

and to use the single curve of L/L_0 against c/h appropriate to small values of the lift coefficient. This curve is shown on a larger scale in Fig. 23 together with the approximate curve according to equation (15.3). The agreement is quite satisfactory, and the error of the

approximate formula does not exceed 2 per cent. of the lift in the range of c/h shown in this figure, but for larger values of c/h it would be advisable to use Rosenhead's accurate curves.

A comparison of Figs. 21 and 23 shows that the interference is far greater in a free jet than in a closed tunnel. Thus when the chord of the wing is half the height of the tunnel, the lift is increased by 9½ per cent. in a closed tunnel and is reduced by 43 per cent. in a free jet. This large difference is due mainly to the downward deflection of the free jet behind the wing, though the correction due to the curvature of the flow in a free jet is also double that in a closed tunnel.

Throughout this analysis it has been assumed that the wing is placed in the centre of the stream, but Rosenhead²⁵ has also given results for a wing whose mid point is at a distance a from the axis of the stream. The method of images can also be used to determine the interference due to the induced curvature of the stream in this case, and the approximate formula for the lift is

$$L_0 = 1 - \frac{\pi^2}{16} \left(\frac{c}{h}\right)^2 \left(\sec^2 \frac{\pi a}{h} - \frac{1}{3}\right) \dots \dots (15.4)$$

Experimental confirmation of all these theoretical formulae for tunnel interference is lacking at present, apart from some tests at Göttingen²¹ where a series of aerofoils were tested in a free jet with the ends of the wings adjoining two vertical walls normal to the span. According to the formula (14.5) the induced drag of the wings should have been equal to that of a wing of aspect ratio 4.4, whilst an analysis of the experimental results suggested an equivalent aspect ratio of 4.1. This difference of 7 per cent. in the induced drag is not unduly large, and it is ascribed by Prandtl²¹ to the fact that the free surface of the jet was curved instead of horizontal, as assumed in the theoretical analysis.

PART 3

Symmetrical Bodies

16. *General discussion.*—The problem of the interference experienced by a body, on which the resultant force is a drag without any cross-wind or lift component, differs noticeably from that of a lifting wing. When considering the behaviour of a wing in a wind tunnel it is legitimate to base the analysis on the assumption of a perfect fluid and to ignore the frictional drag on the surface of the wing, but this course is no longer possible with symmetrical bodies since their drag depends essentially on the departure from these ideal conditions. The problem is, therefore, inevitably more complex, a purely theoretical solution of the problem is impossible, and it is necessary to rely partly on empirical factors derived from the analysis of appropriate experimental results.

The general nature of the interference experienced by a symmetrical body has been discussed briefly in Section 1. The interference is of a complex nature and it is convenient to consider in turn the following three aspects of the problem:—

- (1) The direct constraint of the boundary of the air stream on the flow past the body.
- (2) The additional constraint arising from the existence of a wake of reduced velocity behind the body.
- (3) The effect of a gradient of pressure along the axis of the wind tunnel.

It is now necessary to consider these three elements of the problem more precisely and to derive formulae for the magnitude of the interference experienced by a body.

The direct constraint due to the boundary of the air stream arises because rigid walls prevent free lateral expansion of the flow past the body and because free boundaries impose the condition of uniform pressure at the boundary. This type of constraint would occur under the ideal conditions of a perfect fluid, and it is possible to represent the boundary conditions by the introduction of an appropriate system of images, similar to those used in the problem of a lifting wing. Owing to the presence of these images the body experiences an induced interference velocity, but the drag of a body in a perfect fluid is zero and it will remain zero also when subjected to this constraint. If, however, we pass to the actual conditions, we may conclude, as a first approximation, that a body in a wind tunnel will experience an effective velocity which is the algebraic sum of the undisturbed velocity and of this induced velocity, and that the actual drag will be proportional to the square of this effective velocity. Thus the estimate of this first type of tunnel interference is based on the calculation of the induced velocity due to the appropriate system of images in a perfect fluid. As in the case of a wing, the induced velocity will really have different values at different points of the body, but it will usually suffice to calculate the induced velocity at some typical point and to assume that the whole body is subjected to this modified velocity.

The second type of constraint, due to the wake of reduced velocity behind a body, is unimportant for a good streamline body but is the dominant factor for a bluff body. The existence of this wake implies that the velocity outside the wake in a closed tunnel must be higher than the mean velocity in front of the body in order to maintain continuity of flow. Consequently the pressure of the wake is reduced below its value in an unlimited stream, and this reduced pressure reacts back on the body to cause an increased drag. This type of interference occurs only in a closed tunnel and is absent in a free jet where the whole jet can expand laterally behind the body and so maintain the same pressure behind and in

front of the body. It is possible to obtain theoretically an expression for this constraint, but it is necessary to rely on experimental results to determine an empirical factor owing to insufficient knowledge of the nature of the wake behind different types of body.

The third type of interference arises in practice owing to the development of the boundary layer along the walls of a closed wind tunnel, which leads to a gradual increase of velocity along the axis of the tunnel. Any body is, therefore, tested in a slightly convergent stream with a falling pressure gradient, and the body experiences an increased drag owing to the drop of static pressure from nose to tail. This pressure gradient correction is most important for good streamline bodies whose drag is low, and is relatively unimportant for bluff bodies of high drag. It is, therefore, legitimate to calculate the magnitude of this correction from the ideal conditions of a perfect fluid. The magnitude of the pressure gradient must be measured in the wind tunnel itself, with no body or obstruction in the stream, since its value depends in part on any leakage of air through cracks in the walls or through openings essential to the conduct of experiments. It is important that the pressure gradient should be measured with these openings adjusted as during the test of the body. No pressure gradient is to be anticipated in a free jet, though the same method of correction will apply if such a pressure gradient does occur, and the pressure gradient can be eliminated in a closed tunnel by giving the boundary walls a small angle of divergence down stream.

The detailed analysis of the pressure gradient correction will be deferred to Section 19. The other two types of interference will be considered in conjunction, firstly for the relatively simple problem of two-dimensional motion and then for the more general condition of three-dimensional motion.

17. Two Dimensions.—Consider a symmetrical body, whose maximum thickness is t and whose length or chord is c , lying along the axis of a closed channel of breadth h as shown in Fig. 24. Clearly the necessary boundary conditions will be satisfied if we assume an infinite column of such bodies, spaced at intervals h apart, and the interference experienced by the body can be calculated as the induced velocity of this system of images. In this calculation we may assume the ideal conditions of a perfect fluid and can express the complex potential of the flow past the body in an unlimited stream in the form

$$w = Vz + \frac{A_1}{z} + \frac{A_2}{z^2} + \dots \quad (17.01)$$

The first term of this expression represents the uniform stream of velocity V , and the remaining terms represent the distortion of the flow caused by the body. At a large distance from the body it will suffice to retain only the first of these terms, since the others

will be relatively unimportant, and thus the disturbance of the flow caused by any symmetrical body at a large distance from itself can be represented by the single term

$$w_1 = \frac{A_1}{z} = \frac{\mu}{2\pi z} \quad \dots \quad (17.02)$$

where μ is the strength of a doublet, directed against the undisturbed stream. Now a circular body of radius a is represented by a doublet of strength $2\pi a^2 V$, and hence the approximation of representing the interference of any body by a formula of the type (17.02) implies that the body may be replaced by an equivalent circle of radius $\sqrt{A_1/V}$. It is convenient now to write

$$\mu = 2\pi A_1 = \frac{\pi}{2} \lambda^2 V \quad \dots \quad (17.03)$$

so that the body of thickness t is replaced by an equivalent circle of diameter $t\sqrt{\lambda}$. The disturbance of the flow caused by the body at a large distance from itself is then given by the equation

$$w_1 = \frac{\lambda V t^2}{4z}$$

Returning now to the problem of a symmetrical body in a closed channel, each image of the infinite series is replaced by the equivalent circle and the induced velocity due to this system of images is calculated as follows. The image at distance $n h$ from the body gives the induced velocity

$$u_1 = \frac{\lambda V t^2}{4n^2 h^2}$$

and the total induced velocity is therefore

$$u_1 = \frac{\lambda V t^2}{2h^2} \sum_1^{\infty} \frac{1}{n^2} = \frac{\pi^2}{12} \left(\frac{t}{h}\right)^2 \lambda V \quad \dots \quad (17.04)$$

The interference experienced by a symmetrical body in a free jet of breadth h can be calculated in a similar manner. The only modification of the analysis is that the images are now alternately negative and positive, and hence

$$u_1 = \frac{\lambda V t^2}{2h^2} \sum_1^{\infty} \frac{(-1)^n}{n^2} = -\frac{\pi^2}{24} \left(\frac{t}{h}\right)^2 \lambda V \quad \dots \quad (17.05)$$

In each case the body experiences an effective velocity $(V + u_1)$ and its drag in the channel may be expected to vary as the square of this velocity. Thus we may write

$$\frac{u_1}{V} = \tau \lambda \left(\frac{t}{h}\right)^2 \quad \dots \quad (17.06)$$

and the ratio of the drag in the wind tunnel to its value in an unlimited stream is

$$\frac{D}{D_0} = \left\{ 1 + \tau \lambda \left(\frac{t}{h} \right)^2 \right\}^2 \quad \dots \quad (17.07)$$

Also, since higher powers of t/h have been neglected in the analysis, we can adopt the simpler formula

$$\frac{D}{D_0} = 1 + 2\tau \lambda \left(\frac{t}{h} \right)^2 \quad \dots \quad (17.08)$$

In these formulae λ is a non-dimensional factor depending only on the shape of the body, whilst τ depends on the nature of the boundaries of the stream. We have

$$\left. \begin{aligned} \text{Rigid walls, } \tau &= \frac{\pi^2}{12} = 0.822 \\ \text{Free jet, } \tau &= -\frac{\pi^2}{24} = -0.411 \end{aligned} \right\} \quad \dots \quad (17.09)$$

This method of analysing the problem of the interference experienced by a symmetrical body in a channel is due to Lock³⁴, who has also calculated the values of the factor λ for the following four shapes of body:—

- (1) Joukowski section, with cusp at trailing edge.
- (2) Modified Joukowski section, with finite angle at trailing edge.
- (3) Ellipse.
- (4) Rankine oval, the form due to a source and sink at a finite distance apart.

A simple formula for the factor λ is obtained only in the case of the ellipse, or which

$$\lambda = \frac{1}{2} \left(1 + \frac{c}{t} \right) \quad \dots \quad (17.10)$$

The values of λ , as a function of the fineness ratio c/t , for the four types of body are shown in Fig. 25. The values increase with the fineness ratio and with the bluntness of the body, and all four curves pass through the point corresponding to a circle. The shapes of the four types of body are shown in Fig. 26.

Lock³⁴ has also compared his approximate results for the Rankine ovals with some more accurate calculations by Fage³³, and he concludes that the error of the approximate results is less than 0.5 per cent. if the fineness ratio is less than 5, and for greater fineness ratios if the length of the body is less than the breadth of the channel. The approximate formulae should therefore remain

valid in all practical applications. It is generally possible to estimate the value of λ with sufficient accuracy by interpolation between the curves of Fig. 25. If a more reliable value of λ is required and if the theoretical flow past the body is known, the complex potential function should be expressed in the form (17.01) and the value of λ deduced by means of equation (17.03). Alternatively, if the actual pressure distribution round the body has been determined experimentally, the value of the velocity q at the surface can be calculated by means of Bernoulli's equation and the effective doublet strength of the body can then be derived by evaluating the integral

$$\mu = \int 2qy \, ds$$

or

$$\lambda = \frac{4}{\pi} \int \frac{q}{V} \frac{y \, ds}{t^2} \quad \dots \quad (17.11)$$

where the integral is taken along the upper surface of the body from leading to trailing edge.

On comparing their theoretical formulae with the experimental evidence available, both Fage³³ and Lock³⁴ found it necessary to introduce an empirical factor K , since the observed tunnel interference was greater than that predicted by the theory. The value of K was only slightly greater than unity for a thin streamline body but became very large for bluff bodies. The need of such an empirical correction has been ascribed by the present author³⁷ to the neglect of another type of tunnel constraint which arises owing to the existence of a wake of reduced velocity, particularly behind a bluff body. The nature of this constraint can be appreciated most readily by considering the case of a flat plate with discontinuous flow and with a wake of fluid at rest as shown in Fig. 27. In order to maintain continuity of flow the velocity W outside the wake must exceed the tunnel velocity V , and hence the pressure in the wake is reduced by the constraint of the tunnel walls. This reduced pressure acting on the rear of the plate gives an increased drag, whose magnitude depends mainly on the ratio of the width of the wake to the width of the channel. The theoretical results for this problem of a flat plate in a closed channel are summarised in Table 19, and an inspection of the last two columns of this table indicates that the drag of the plate in the channel is sensibly the same as that of the plate in an unlimited stream of velocity W .

TABLE 19

Flat plate, discontinuous flow

t/h	s/h	k_D	$0.44 \frac{h^2}{(h-s)^2}$
0	0	0.44	0.44
0.061	0.233	0.75	0.75
0.102	0.300	0.90	0.90
0.149	0.363	1.09	1.08
0.201	0.423	1.34	1.32
0.443	0.636	3.44	3.32

Actually, a bluff body does not give this type of discontinuous flow, but develops a periodic eddying wake of reduced velocity. It seems probable, however, that there will be a tunnel constraint of the form

$$D = D_0 \left(1 - \eta \frac{t}{h}\right)^{-2} \dots \dots \dots (17.12)$$

where ηt is the effective width of the wake as regards this type of tunnel interference. This correction is additional to the induced velocity correction considered previously, and although the correct method of combining the two corrections is uncertain, it is suggested that the most suitable formula for representing the total tunnel interference on a symmetrical body is

$$\frac{D}{D_0} = \left\{1 + \tau \lambda \left(\frac{t}{h}\right)^2\right\}^2 \left(1 - \eta \frac{t}{h}\right)^{-2} \dots (17.13)$$

To a first approximation the wake correction is proportional to t/h and the induced velocity correction to $(t/h)^2$. Moreover, we may anticipate that the wake correction will be most important for bluff bodies, which create wide wakes, and that the induced velocity correction will be most important for bodies of high fineness ratio, for which the value of λ is large. Finally, it is important to remember that the wake correction occurs only in a closed channel and that it is essentially zero in a free jet.

The empirical factor K , introduced by Fage and Lock, was necessary owing to the omission of the second factor of the formula (17.13) in their analysis. In this latter formula there is still an empirical factor η , since our knowledge of the conditions behind a body is insufficient for any calculation of the effective width of the wake. Values of this factor η have been derived by an analysis²⁷ of the available experimental evidence, and were found to lie on a single curve when plotted against the fineness ratio of the body. This curve is reproduced in Fig. 28, and numerical values, taken

from the curve, are given in Table 20. The bodies, used in the experimental investigation, were three Joukowski sections, a Rankine oval, an ellipse, a circle and a flat plate. It is perhaps

TABLE 20

Values of η

c/t η	0	1	2	4	6	8
	1.00	0.30	0.22	0.13	0.08	0.06

rather surprising that all the values of η should lie on a single curve, since it would be anticipated that a bluff body, such as an ellipse or oval, would give a higher value of η than a Joukowski section of the same fineness ratio. The experimental evidence is, however, rather scanty, and the value of η depends on the small difference between two observed drag coefficients. The single curve nevertheless represents the experimental evidence which was obtained with special care, and any deviation of the value of η from this curve for different shapes of body may be expected to be negligible in practice. Fig. 29 shows a comparison between the observed drag of a Joukowski section of fineness ratio 3 and the curve predicted by means of the formula (17.13) using the values $\lambda = 1.77$ and $\eta = 0.17$. The wake correction to a flat plate normal to the stream, as given by this method of analysis, agrees closely with that derived in another investigation³⁰ by considering the behaviour of the vortex street behind the body in a channel of finite breadth.

18. *Three dimensions.*—The interference experienced by a body of revolution with its axis along the central axis of a wind tunnel is of the same nature as in the two-dimensional problem. In a free jet the interference can be estimated by calculating the induced velocity of the appropriate image system which satisfies the necessary boundary condition and in a closed tunnel there is an additional interference due to the choking action of the wake behind the body. No new features arise in the problem, but the analysis becomes far more complex than in the simpler problem of two-dimensional motion.

The problem of the induced velocity experienced by the body has been considered by Lock³¹, who expresses this induced velocity in the form

$$\frac{u_1}{V} = \tau \lambda \left(\frac{S}{C}\right)^{3/2} \dots \dots \dots (18.1)$$

where C is the cross-sectional area of the tunnel, S is the maximum cross-sectional area of the body, τ is a factor depending on the shape of the tunnel and the nature of the boundary, and λ is a factor

depending on the shape of the body. The definition of λ is such that in the image systems a body of maximum diameter t is replaced by an equivalent sphere of diameter $t\lambda^{1/3}$.

The boundary conditions for a rectangular tunnel or jet can be represented by the introduction of a doubly infinite set of images, and each of these images can be regarded approximately as a doublet of strength μ , where

$$\mu = \frac{\pi}{4} \lambda t^3 V \dots \dots \dots (18.2)$$

For a closed rectangular tunnel all the doublets are of the same sign and they occur at the points (mb, nh) where b and h are the sides of the tunnel and (m, n) are any pair of positive or negative integers. The induced velocity due to one of these image doublets is

$$u_1 = \frac{\mu}{4\pi (m^2 b^2 + n^2 h^2)^{3/2}} \dots \dots (18.2)$$

and the total induced velocity is obtained by the double summation of this expression for all positive and negative integral values of m and n , excluding the pair $(0, 0)$. For a free jet the signs of the doublets alternate in both rows and columns, and the expression (18.2) receives a factor $(-1)^{m+n}$. Lock³⁴ has evaluated these summations for closed and free square tunnels, and for a closed duplex tunnel ($b = 2h$), and the resulting values of the factor τ are given in Table 21 below.

The analysis for a circular tunnel is even more complex. Lamb²⁹ has considered the interference experienced by a Rankine ovoid, which is the body formed by a source and sink at a finite distance apart, in a closed circular tunnel, and Lock³⁴ has developed a similar analytical treatment for a free jet. The series of Bessel functions which occur in this analysis have been reduced to a form more suitable for numerical computation by Watson³⁵, and the values of τ deduced from this analysis are included in Table 21. The values of τ for square and circular tunnels are not very different, and the value of τ in a free jet is approximately one quarter of that in the corresponding closed tunnel.

TABLE 21
Values of τ

Shape of tunnel.	Closed tunnel.	Free jet.
Circle	0.797	-0.206
Square	0.809	-0.238
Duplex	1.03	

Lock³⁴ has calculated the values of λ for two shapes of body, the Rankine ovoid and the spheroid, and these results are shown in Fig. 30 against the fineness ratio of the body. The value of λ can be derived from any body, round which the theoretical flow is known, by considering the velocity on the axis of symmetry at a great distance from the body, which is of the form

$$u = -\frac{\mu}{2\pi r^3} = -\frac{\lambda}{8} \left(\frac{t}{r}\right)^3 V \dots (18.3)$$

where r is the distance from the body. Alternatively, if the velocity q along the surface of the body can be deduced from the observed pressure distribution, the value of λ can be deduced by evaluating the integral

$$u = -\int \frac{q y^2 ds}{2r^3}$$

or

$$\lambda = 4 \int \frac{q y^2 ds}{V t^3} \dots \dots (18.4)$$

where the integral is taken along any generator of the body from nose to tail.

The constraint represented by the induced velocity u_1 , as given by equation (18.1) must be increased, as in two-dimensional motion, by a term representing the effect of the wake behind the body. Corresponding to the formula (17.13) for two-dimensional motion, we have in the more general case of three-dimensional motion

$$\frac{D}{D_0} = \left\{ 1 + \tau \lambda \left(\frac{S}{C}\right)^{3/2} \right\}^2 \left(1 - \eta' \frac{S}{C} \right)^{-2} \dots (18.5)$$

where η' is an empirical factor representing the effective size of the wake.

The experimental results on two streamline bodies have been analysed by Lock and Johansen³⁶ to check the theoretical prediction of the tunnel constraint as given by the induced velocity u_1 . This analysis was difficult owing to the small values of the drag coefficient, owing to the existence of an important pressure gradient correction, and owing to the difficulty of maintaining the same conditions in the boundary layer of the body under different experimental conditions. The experiments do not therefore provide a very reliable check on the accuracy of the calculated induced velocity, but it is noticeable that Lock and Johansen did not find it necessary to introduce any empirical factor K , as in the analysis of the experiments in two-dimensional motion. It would appear therefore that the wake correction was unimportant. This result is due partly to the fact that the wake can contract in two directions and will therefore

be relatively less important than in two-dimensional motion. In the absence of more reliable information we may assume that, for a given fineness ratio,

$$\eta' = \eta^2 \dots \dots \dots (18.6)$$

The largest body used by Lock and Johansen had a fineness ratio 3 and a cross-sectional area 0.06C, and on the basis of the formulae (18.5) and (18.6) the wake correction to the drag would be only 0.35 per cent, which is quite negligible. Thus we may accept these formulae as giving a sufficiently reliable estimate of the tunnel interference due to induced velocity and wake constraint, remembering that the wake constraint is absent in a free jet and negligible for a good streamline body in a closed tunnel.

Lock and Johansen²⁶, during the course of their analysis of the experimental results on two streamline bodies, also considered the effect of the tunnel constraint on the pressure distribution round a body. The total drag of the bodies did not provide a suitable test of the theoretical formulae for tunnel interference owing to the sensitivity of the frictional drag to changes in the nature of the flow in the boundary layer, whereas the pressure distribution is not seriously modified by these changes. On the assumption that a body subjected to a velocity V in a wind tunnel behaves in the same manner as in an unlimited stream of velocity $(V+u_1)$, the appropriate correction to the observed pressure p at any point of the body appears to be

$$p_1 = p + \frac{1}{2} \rho \{(V+u_1)^2 - V^2\} \dots \dots (18.7)$$

where p_1 is the corresponding pressure in the unlimited stream. This formula gives the correct stagnation pressure at the nose of the body, and equal values for the integrated drag in the wind tunnel and in the unlimited stream. If the pressures are expressed non-dimensionally by the formulae

$$p = k_p \rho V^2$$

$$p_1 = k_p' \rho (V+u_1)^2$$

the formula for the tunnel interference becomes

$$k_p' = \frac{1}{2} - \left(\frac{V}{V+u_1} \right)^2 \left(\frac{1}{2} - k_p \right) \dots \dots (18.8)$$

or approximately

$$k_p' = k_p + \frac{u_1}{V} (1 - 2k_p) \dots \dots (18.9)$$

During the course of the analysis Lock and Johansen found that this correction to the local pressure was more important than that due to the pressure gradient, which will be considered in Section 19, whereas the correction to the total drag was due mainly to the

pressure gradient. The analysis of the pressure distributions round two bodies of the same shape but of different size was in satisfactory agreement with this formula for the tunnel interference.

19. *Pressure gradient.*—The origin of the pressure gradient along the axis of a closed wind tunnel has been discussed previously in Section 16, and it is now necessary to consider the magnitude of the force experienced by a body due to this pressure gradient. The existence of this pressure gradient drag was realised at an early date by Pannell and Campbell²⁸, and after some discussion Pannell, Jones and Pell²⁷ adopted, as the correction to be applied to the observed drag, the horizontal buoyancy of the body, which is the product of the volume of the body and the pressure gradient. The fact that this horizontal buoyancy is only an approximation to the true pressure gradient drag was demonstrated by Munk²⁸ in a brief note at the end of a paper dealing with some miscellaneous aerodynamic problems. Munk's analysis showed that the pressure gradient drag was equal to the product of the pressure gradient and a certain effective volume, which was greater than the actual volume by an amount which increased as the fineness ratio of the body decreased. The problem has been discussed in greater detail more recently by Taylor³² and the present author³¹, who proved that the effective volume of the body, as regards the pressure gradient drag, is the sum of the actual volume of the body and of the volume corresponding to the virtual mass of the body in accelerated motion along its axis.

The truth of this general proposition can be established by a simple physical argument without entering into the details of the mathematical analysis. A body in a closed wind tunnel is subjected to a flow which is accelerating in the direction of motion and the consequent variation of static pressure is

$$\frac{dp}{dx} = -\rho V \frac{dV}{dx} \dots \dots (19.01)$$

The body, subjected to this pressure gradient, experiences a horizontal buoyancy which is equivalent to a drag force

$$D_1 = -A \frac{dp}{dx}$$

where A is the volume of the body, but in addition the body has the acceleration $\frac{dV}{dt}$ or $V \frac{dV}{dx}$ relative to the surrounding fluid and hence experiences an additional drag force

$$D_2 = \rho A' V \frac{dV}{dx} = -A' \frac{dp}{dx}$$

where $\rho A'$ is the virtual mass of the body for accelerated motion along its axis. Thus the total drag of the body due to the pressure gradient of the stream is

$$D = - (A + A') \frac{dp}{dx} = - A'' \frac{dp}{dx} \quad \dots (19.02)$$

This is the general result which was established by Taylor³² by a detailed mathematical analysis of the problem.

The value of the virtual volume A' can be determined by the standard methods of hydrodynamics, when the theoretical flow round the body is known, but the following simple method of analysis has the advantage of expressing the virtual volume in terms of the coefficient λ , introduced in the earlier analysis in the formula for the induced velocity experienced by a body. The problem of a body in a slightly divergent flow is equivalent to that of the body in the presence of a source at a large distance in front of the body as shown in Fig. 31. The resultant force on the combined system of body and source is essentially zero, and hence the force on the body is equal and opposite to the force on the source. But the force on a source of strength m , subjected to a velocity u , is

$$X = - \rho m u$$

and hence the drag of the body in the slightly divergent stream is

$$D = \rho m u \quad \dots (19.03)$$

where u is the velocity at the source due to the presence of the body. Also, if the source is at a large distance R from the body, the influence of the body is the same as that of a doublet of strength μ directed towards the source.

To proceed further with the analysis it is necessary to consider separately the motion in two and in three dimensions. In two-dimensional motion, according to the analysis of Section 17, the body can be replaced by an equivalent circle of diameter $t\sqrt{\lambda}$, where t is the maximum width of the body and λ is a factor depending on the shape of the body. The corresponding strength of the doublet is

$$\mu = \frac{\pi}{2} \lambda t^2 V$$

whilst the strength of the source will be

$$m = 2\pi R V$$

The velocity experienced by the source, due to the presence of the body, is

$$u = - \frac{\mu}{2\pi R^2}$$

and hence, according to the equation (19.03), the drag of the body is

$$D = - \frac{\pi}{2} \lambda t^2 \frac{\rho V^2}{R}$$

Now the velocity along the axis due to the source is

$$u = \frac{VR}{R+x}$$

and hence the pressure gradient in the neighbourhood of the body is

$$\frac{dp}{dx} = - \rho V \frac{dV}{dx} = \frac{\rho V^2}{R}$$

Thus the drag of the body is

$$D = - \frac{\pi}{2} \lambda t^2 \frac{dp}{dx} \quad \dots (19.04)$$

and, by comparison with the fundamental formula (19.02), the effective area of the body required in the formula for the pressure gradient correction is

$$A'' = \frac{\pi}{2} \lambda t^2 \quad \dots (19.05)$$

In three-dimensional motion the same method of analysis can be used with the following slight modifications. The strengths of the doublet and source are respectively

$$\mu = \frac{\pi}{4} \lambda t^3 V$$

and

$$m = 4\pi R^2 V$$

The velocity experienced by the source, due to the presence of the body, is now

$$u = - \frac{\mu}{2\pi R^3}$$

and the drag of the body is

$$D = - \frac{\pi}{2} \lambda t^3 \frac{\rho V^2}{R}$$

whilst the pressure gradient in the neighbourhood of the body in three-dimensional motion is

$$\frac{dp}{dx} = \frac{2\rho V^2}{R}$$

Thus finally the drag of the body is

$$D = -\frac{\pi}{4} \lambda t^3 \frac{dp}{dx} \quad \dots \quad (19.06)$$

and the effective volume required in the formula for the pressure gradient correction is

$$A'' = \frac{\pi}{4} \lambda t^3 \quad \dots \quad (19.07)$$

The determination of the coefficient λ has been considered previously and values for some types of body are given in Figs. 25 and 30. In particular for an ellipse we have, according to equation (17.10),

$$\lambda = \frac{1}{2} \left(1 + \frac{c}{t} \right)$$

whilst the area of the ellipse is

$$A = \frac{\pi}{4} ct$$

Hence from equation (19.05),

$$A'' = A \left(1 + \frac{t}{c} \right) \quad \dots \quad (19.08)$$

Thus the ratio of the effective area A'' to the actual area A increases as the fineness ratio of the ellipse decreases. For thin streamline bodies the effective area A'' will be only slightly greater than the actual area A , but the ratio of these two areas increases to 2.0 for a circle. Similar results can be derived in three dimensions, and in particular the effective volume of a sphere is 1.5 times the actual volume.

Alternatively the equations (19.05) and (19.07), which give the relationship between the coefficient λ and the effective area or volume of the body in two and three dimensions respectively, can be used to determine the values of λ when the virtual mass of the body is known. As the fineness ratio of a body increases the ratio of A'' to A tends to unity, and therefore as a first rough approximation for streamline bodies of high fineness ratio we may take

$$A'' = A$$

Consequently the first approximation to the value of λ in two dimensions is

$$\lambda = \frac{2A}{\pi t^2} \quad \dots \quad (19.09)$$

whilst the corresponding approximation in three dimensions is

$$\lambda = \frac{4A}{\pi t^3} \quad \dots \quad (19.10)$$

By comparison with the true values for an ellipse and a spheroid, it appears that this approximation is more accurate in three than in two dimensions. These approximate formulae should be used only when more reliable values are not available.

The effect of the pressure gradient in a wind tunnel on the pressure distribution round a body has also been considered by Lock and Johansen³⁶, who have expressed the correction in the form

$$\delta p = \frac{1}{2} Y c \frac{dp}{dx} \quad \dots \quad (19.11)$$

where c is the length of the body and Y is a function of position over the surface of the body, depending on the shape of the body. This correction must be added to the observed pressure to obtain the corresponding pressure in a uniform stream. Lock and Johansen calculated the values of Y for a spheroid from the exact solution of the flow past the body in a convergent stream, and the curves of Y against the coordinate x/c measured along the axis of the spheroid from its nose for two values of the fineness ratio are shown in Fig. 32. When the body is not a spheroid they suggest that these same values of Y may be used as a first approximation to estimate the correction to the pressure distribution over the body.

In the experiments analysed by Lock and Johansen the correction to the local pressures due to the pressure gradient is less than that due to the induced velocity as discussed in Section 18, though the correction to the total drag is due mainly to the pressure gradient.

As regards the usual magnitude of the pressure gradient in a closed wind tunnel, it has already been explained that the drop of pressure along the axis of the tunnel is due partly to the development of the boundary layer along the walls and partly to the leakage of air into the tunnel through cracks or openings in the walls. For a square tunnel of side h it is convenient to express the pressure gradient in the form

$$\frac{dp}{dx} = -k \frac{\rho V^2}{h} \quad \dots \quad (19.12)$$

The value of the non-dimensional coefficient k for a tunnel with air-tight walls is then of the order 0.008, and rises to 0.020 for a tunnel with a moderate amount of leakage through the walls. The pressure gradient can be eliminated by giving a small angle of divergence to the walls, but its value must be determined specially in any experiment where the correction due to the pressure gradient may be important.

PART 4
Airscrews

20. *General Discussion.*—The interference experienced by an airscrew in a wind tunnel resembles that part of the interference experienced by a symmetrical body which is due to the existence of a wake of reduced velocity behind a body. An airscrew, when giving a positive thrust, creates a wake or slipstream of increased velocity. If the flow is confined between the rigid walls of a closed tunnel, the condition of continuity of flow leads to a reduced velocity and increased pressure of the fluid surrounding the wake, and these modified conditions behind the airscrew react back to change the relationship between the thrust and rate of advance of the airscrew for a given rate of rotation. In a free jet, on the other hand, the jet surrounding the slipstream can contract in order to maintain the same velocity and pressure as in the undisturbed stream in front of the airscrew, and there is no appreciable tunnel interference on the behaviour of the airscrew.

The existence of a tunnel constraint on the behaviour of an airscrew in a closed tunnel was appreciated at an early date by Bramwell, Relf and Bryant³⁹, who determined an empirical equivalent free airspeed, corresponding to the observed speed in the wind tunnel far in front of the airscrew, by comparing the thrust of the airscrew in the wind tunnel with the thrust measured on a whirling arm. A theoretical formula for this equivalent free airspeed was later derived by Wood and Harris⁴⁰. The validity of this theoretical formula and the absence of any appreciable interference on the behaviour of airscrews of moderate size in a free jet have been checked by special experiments which are discussed in Section 22. A discussion of these experimental results and of the whole problem of wind tunnel interference on airscrews is also the subject of a report by Glauert and Lock⁴¹.

The use of an equivalent free airspeed to represent the tunnel interference is valid only when the airscrew is operating at a positive rate of advance or when it is acting as a windmill with a slipstream of conventional type but reduced velocity. There are, however, some states of operation of an airscrew which cannot be treated in this manner. In particular the static condition (zero rate of advance) cannot be reproduced in a closed wind tunnel, since the airscrew itself will induce a flow through the tunnel. This same difficulty will arise to a smaller degree even in an open jet tunnel with a closed return circuit but results obtained in a free jet are probably more reliable than those obtained in a closed tunnel. The only satisfactory method of determining the static thrust of an airscrew is, however, to conduct the experiment in a large room.

Even greater difficulties arise in the determination of the behaviour of an airscrew at low negative rates of advance. The

airscrew then either operates in the vortex ring state with flow through the disk opposed to the general stream, or develops a turbulent wake differing essentially from a conventional slipstream. There is no satisfactory method of correcting results obtained in a closed wind tunnel in these extreme conditions of operation of an airscrew, and the experimental evidence suggests that the tunnel constraint may be large⁴². In a free jet the tunnel constraint on these extreme conditions of operation of an airscrew is also unknown, but it is probably small. The subsequent analysis and discussion will be confined to the usual operating conditions at a positive rate of advance when the airscrew develops a positive thrust and a conventional slipstream.

In practice, an airscrew operates in conjunction with a body, either as a tractor or as a pusher. The problem of the tunnel interference then becomes more complex since the constraint is due partly to the airscrew and partly to the body. Frequently the body is so small that its contribution to the tunnel constraint may be ignored, but when the body is large it is necessary to rely on certain empirical methods of correcting for the tunnel constraint.

21. *Closed wind tunnels.*—The theoretical method of calculating the interference experienced by an airscrew in a closed wind tunnel is due to Wood and Harris⁴⁰, and the resulting equations have been reduced to a form more suitable for numerical computation by the present author²². The fundamental basis of the method is to replace the airscrew by an actuator disk, as in the classical momentum theory of an airscrew, to ignore the rotation of the slipstream due to the torque of the airscrew, and to consider the flow in the distant wake as modified by the constraint of the tunnel walls. The flow is then of the type illustrated in Fig. 33, where V is the tunnel velocity far in front of the airscrew, u is the velocity through the airscrew disk and u_1 is the slipstream velocity, whilst w and w_1 are the corresponding velocities of the flow surrounding the slipstream. The next step in the argument depends on the fact that the thrust given by the blades of an airscrew, at a given rate of rotation, depends only on the velocity u through the disk. Thus in an unlimited stream the airscrew will give the same thrust T as in the wind tunnel if the velocity through the disk has the same value, but this condition will in general correspond to an equivalent free airspeed V' which differs from the tunnel velocity V . The problem to be considered is therefore the determination of the equivalent free airspeed V' corresponding to any given conditions in the wind tunnel.

Now if A is the disk area of the airscrew, the conditions in an unlimited stream are determined by the well known equation

$$T = 2A\rho u(u - V) \quad \dots \dots \dots (21.01)$$

Turning next to the conditions in a wind tunnel, as illustrated by Fig. 33, let C be the cross-sectional area of the tunnel and S that of the slipstream. Then the conditions for continuity of flow are

$$Au = Su_1 \quad \dots \quad (21.02)$$

and

$$CV = Su_1 + (C - S)w_1 \quad \dots \quad (21.03)$$

Secondly the thrust per unit area of the disk is equal to the increase of total pressure head in the slipstream, or

$$T = \frac{1}{2} A \rho (u_1^2 - w_1^2) \quad \dots \quad (21.04)$$

and thirdly, the increase of pressure far behind the airscrew is

$$p_1 - p_0 = \frac{1}{2} \rho (V^2 - w_1^2) \quad \dots \quad (21.05)$$

Finally the momentum equation for the whole flow in the wind tunnel is

$$T - C(p_1 - p_0) = S \rho u_1 (u_1 - V) - (C - S) \rho w_1 (V - w_1) \quad (21.06)$$

These equations suffice to give a complete solution of the problem under consideration. Writing

$$\tau = \frac{T}{A \rho V^2} \quad \dots \quad (21.07)$$

and

$$\alpha = \frac{A}{C} \quad \dots \quad (21.08)$$

to define two non-dimensional quantities whose values are known in any wind tunnel experiment, it is possible theoretically to eliminate the five quantities S, u, u₁, w₁ and (p₁ - p₀) from the first six equations and to derive a relationship of the form

$$\frac{V'}{V} = f(\tau, \alpha)$$

Actually, it is not possible to obtain a simple expression of this form, and it is necessary to calculate the values of V'/V corresponding to chosen values of τ and α by using certain subsidiary variables. Numerical values derived in this manner are given in Table 22 below and are shown graphically in Fig. 34.

In general the ratio α of the disk area A to the tunnel area C is small, and it is therefore legitimate to derive an approximate formula by retaining only the first power of α in the general solution. The approximate formula obtained by Wood and Harris⁴⁰ by this method is

$$\frac{V'}{V} = 1 - \frac{\tau \alpha}{2\sqrt{1+2\tau}} \quad \dots \quad (21.09)$$

and values of the equivalent free airspeed derived from this simple formula do not differ by more than 1 per cent. from the accurate values of Table 22 for the range of values of α and τ given there.

TABLE 22
Values of V'/V

τ =	0.5	1.0	1.5	2.0	2.5	3.0
α=0.05	0.991	0.986	0.981	0.978	0.974	0.972
0.10	0.982	0.971	0.963	0.955	0.949	0.943
0.15	0.973	0.956	0.942	0.931	0.921	0.912
0.20	0.964	0.940	0.922	0.906	0.893	0.882
0.25	0.955	0.924	0.899	0.881	0.865	0.851

It is possible to derive the approximate formula (21.09) directly in the following simple manner. In free air at a rate of advance V we have the equation

$$T = \frac{1}{2} A \rho (u_1^2 - V^2)$$

and hence

$$u_1 = V \sqrt{1+2\tau} \quad \dots \quad (21.10)$$

Also

$$\frac{S}{A} = \frac{u}{u_1} = \frac{u_1 + V}{2u_1} = \frac{1 + \sqrt{1+2\tau}}{2\sqrt{1+2\tau}} \quad \dots \quad (21.11)$$

As a first approximation we can assume that these two relationships remain true in a wind tunnel when the ratio α is small, and then from the equation of continuity (21.03) we obtain

$$(C - S)(V - w_1) = S(u_1 - V)$$

or approximately

$$\frac{V - w_1}{V} = \frac{S}{C} \frac{u_1 - V}{V} = \frac{\tau \alpha}{\sqrt{1+2\tau}} \quad \dots \quad (21.12)$$

by virtue of the equations (21.10) and (21.11). Finally, by analogy with other work on wind tunnel interference, we may assume that the effective velocity V' experienced by the airscrew in the wind tunnel is the mean of the velocities V and w₁ for before and behind the airscrew. Thus we obtain

$$\frac{V - V'}{V} = \frac{\tau \alpha}{2\sqrt{1+2\tau}} \quad \dots \quad (21.13)$$

which is identical with the approximate formula (21.09) derived from the more detailed analysis of the problem.

Before leaving this problem it is interesting to examine the value of the velocity w of the surrounding stream in the plane of the airscrew, since this velocity is occasionally used as the basis of an empirical correction to the wind tunnel observations. From the equation of continuity

$$(C - A)w = CV - Au \dots \dots \dots (21.14)$$

or approximately

$$\frac{V-w}{V} = \frac{A}{C} \frac{u-V}{V}$$

and hence

$$\frac{w}{V} = 1 - \frac{a}{2} (\sqrt{1+2\tau} - 1) \dots \dots (21.15)$$

To the first order of τ the value of this velocity w is equal to that of the equivalent free airspeed V' as given by equation (21.09) but for larger values of τ the tunnel interference will be over-estimated if the velocity w is used instead of the equivalent free airspeed V' . On the other hand this theoretical estimate of the velocity w is based on the assumption of a uniform velocity of the stream outside the airscrew, whereas in fact the velocity may vary from the tip of the airscrew to the walls of the tunnel. The possibility of using measurements of the velocity in the plane of the airscrew as a measure of the equivalent free airspeed has been examined by Fage⁴¹ who measured the radial distribution of axial velocity in three planes adjacent to that of the airscrew disk. In a plane immediately behind the airscrew the mean velocity outside the slipstream agreed approximately with the value of w given by the formula (21.15), but the velocity was increasing from the edge of the slipstream outwards. Apart from a drop on approaching the boundary layer along the walls of the wind tunnel, the velocity in each of the three planes of observation appeared to be tending towards a common limiting value, which agreed closely with the equivalent free airspeed given by the formula (21.09). Consequently this experimental method of measuring the velocity distribution outside the disk of the airscrew provides an alternative method of estimating the magnitude of the tunnel constraint.

22. *Free jets.*—As explained previously in Section 20, it is to be expected that the tunnel constraint on an airscrew in a free jet will be negligibly small since the stream surrounding the slipstream can contract and thus maintain the same velocity and pressure as the undisturbed stream in front of the airscrew. This conclusion, has been confirmed experimentally by Durand³⁹. In one series of experiments he tested four airscrews of diameter 2½, 3, 3½ and 4 ft. respectively in a free jet of diameter 5½ ft. The observed values of the thrust coefficients of these four airscrews showed no

systematic differences, except that the values derived from the 3 ft. airscrew were slightly higher than those given by the other three airscrews. This slight variation was ascribed by Durand to some slight error in shape of the 3 ft. airscrew. In another series of experiments a 3 ft. airscrew was tested in a free jet whose diameter was reduced by successive steps of 6 in. from 5½ to 4 ft. The observed thrust and torque coefficients in the 5½ ft. and 5 ft. jets were identical, those in the 4½ ft. jet were 2½ per cent. higher and those in the 4 ft. jet were 6 to 7 per cent. higher than in the larger jets. From the results of these tests it may be concluded that the interference on an airscrew in a free jet does not become appreciable until the diameter of the airscrew exceeds 60 per cent. or perhaps even 70 per cent. of the diameter of the jet. Thus for all practical purposes the interference experienced by an airscrew in a free jet may be neglected.

The accuracy of the experimental results obtained in a free jet enables a check on the accuracy of the formula for the equivalent free airspeed in a closed tunnel to be obtained by comparing tests on the same airscrew in a closed tunnel and in a free jet. Bramwell's experimental results³⁸, obtained in a closed tunnel and on a whirling arm, are of little value as a real test of the correction formula owing to the smallness of the correction itself and to irregular scattering of the observed values of the thrust coefficient, but the magnitude of the correction is reasonably consistent with the theoretical formula (21.09). A more suitable series of experiments was made by Townend and Warsap⁴⁴ who tested a metal airscrew of diameter 3 ft. in a closed 7 ft. square tunnel for comparison with American tests in a free jet. Unfortunately this series of experiments also does not provide a critical test of the theoretical formula owing to the low thrust of the airscrew and the low ratio of the disk area to the tunnel area (0.145). The comparison is further complicated by a noticeable scale effect in the experimental results at different rates of rotation of the airscrews. Over most of the range of advance-diameter ratio the interference correction was not much greater than the experimental errors, but the authors conclude that the tests show that the corrected results obtained from a 3 ft. airscrew in a 7 ft. closed tunnel agree very closely with tests made in a free jet. The theoretical formula (21.09) can, therefore, be accepted as giving the interference on an airscrew in a closed tunnel with sufficient accuracy for all practical purposes, whilst the interference in a free jet can be ignored completely.

23. *Airscrew and body.*—When an airscrew is mounted in front of a large body the tunnel constraint is due partly to the action of the airscrew and partly to that of the body. No theoretical solution of this complex problem has been obtained, but Fage⁴¹ has proposed the empirical method of measuring the radial distribution of velocity outside the slipstream in planes adjacent to that of the airscrew

disk and so determining the common limiting value as described at the end of Section 21. The validity of this method of determining the equivalent free airspeed has been confirmed by Lock and Bateman⁴² by some special experiments on a small airscrew and body combination in a 4 ft. and in a 7 ft. wind tunnel, and satisfactory agreement was obtained both on effective thrust and on torque when the observed values were corrected for the tunnel constraint by the use of the equivalent free airspeed determined experimentally from the velocity distribution.

The validity of this method of estimating the tunnel interference on an airscrew and body combination would appear to depend essentially on the fact that the drag of the body is only a small fraction of the thrust of the airscrew, and the problem would require reconsideration under different conditions. On the other hand if a complete model aeroplane with airscrew running is placed in a wind tunnel, the airscrew and body will be so small that the tunnel interference may be neglected. The only important tunnel constraint on a complete model aeroplane is that due to the lift of the wings, which has been fully considered in Part I, both as regards the effect on the wings themselves and as regards the tail-setting and angle of downwash.

Lock and Johansen⁴³, in two reports dealing with the pressure distribution over a streamline body with tractor airscrew running, have considered in some detail the very complex tunnel interference, experienced by this combination. No really satisfactory solution of the problem was possible, and it was necessary to use a variety of empirical corrections. The principal sources of the tunnel interference are the drop of static pressure gradient along the axis of the tunnel, the constraint imposed on the airscrew which can be represented by an equivalent free airspeed, and the constraint imposed on the body owing to the constriction of the flow by the walls of the tunnel. To assist in the analysis, observations of the static pressure were made at a distance of 1 ft. from the walls of the tunnel in each state of operation of the airscrew. The true pressure at any point of the body was then assumed to be the excess of the observed pressure over the static pressure near the wall of the tunnel in the same cross-section, since in an unlimited stream this pressure would have the constant value of the atmospheric pressure. The validity of this basis of correction is very doubtful and requires verification by means of experiments with different relative sizes of body and airscrew. As an additional correction the effective velocity experienced by the body as regards the pressure distribution, was chosen to be that corresponding to the observed dynamic pressure at the nose of the body. The equivalent free airspeed experienced by the airscrew was determined from observations of the velocity in the plane of the airscrew, as suggested by Fage⁴¹ and described previously in Section 21, and this same velocity was

used for correcting the total drag of the body, either as observed directly or derived by integration of the pressure distribution. Complex experiments of this nature are not made frequently, but further experimental work is clearly necessary before it will be possible to standardise appropriate methods of correction for the tunnel interference.

REFERENCES

PART I

Wings, Three Dimensions

- (1) L. Prandtl. Tragflügeltheorie, Part 2. Nachrichten der K. Gesellschaft der Wissenschaften zu Göttingen (1919), reprinted in Vier Abhandlungen zur Hydrodynamik und Aerodynamik, by L. Prandtl and A. Betz (Göttingen, 1927).
- (2) H. Glauert. Aerofoil theory. A.R.C., R. & M. 723 (1921).
- (3) H. Glauert. The interference of wind channel walls on the aerodynamic characteristics of an aerofoil. A.R.C., R. & M. 867 (1923).
- (4) L. Prandtl. Experimentelle Prüfung der Berichtigungsformel für Flügel von grosser Spannweite im Luftstrahl der Versuchsanstalt. Ergebnisse der Aerodynamischen Versuchsanstalt zu Göttingen, Vol. 2, p. 17 (1923).
- (5) W. L. Cowley and L. J. Jones. An experimental test of the Prandtl correction for tunnel wall interference. A.R.C., R. & M. 898 (1924).
- (6) H. Glauert and A. S. Hartshorn. The interference of wind channel walls on the downwash angle and the tail-setting to trim. A.R.C., R. & M. 947 (1924).
- (7) G. J. Higgins. The effect of the walls in closed type wind tunnels. N.A.C.A. Report 275 (1927).
- (8) K. Terazawa. On the interference of wind tunnel walls of rectangular cross-section on the aerodynamical characteristics of a wing. Tokyo Imp. Univ., Aero. Res. Inst., Report 44 (1928).
- (9) F. B. Bradfield, K. W. Clark and R. A. Fairthorne. Measurement of maximum lift in closed tunnels of different sizes and in an open jet tunnel. A.R.C., R. & M. 1363 (1930).
- (10) M. Knight and T. A. Harris. Experimental determination of jet boundary corrections for airfoil tests in four open wind tunnel jets of different shapes. N.A.C.A., Report 361 (1930).
- (11) L. Rosenhead. The effect of wind tunnel interference on the characteristics of an aerofoil. Proc. Roy. Soc., A.129, p. 135 (1930).
- (12) T. Theodorsen. The theory of wind tunnel wall interference. N.A.C.A., Report 410 (1931).
- (13) H. Glauert. The interference on the characteristics of an aerofoil in a wind tunnel of circular section. A.R.C., R. & M. 1453 (1931).
- (14) H. Glauert. The interference on the characteristics of an aerofoil in a wind tunnel of rectangular section. A.R.C., R. & M. 1459 (1932).
- (15) H. Glauert. Some general theorems concerning wind tunnel interference on aerofoils. A.R.C., R. & M. 1470 (1932).
- (16) C. B. Millikan. On the lift distribution for a wing of arbitrary plan form in a circular wind tunnel. Trans. American Soc. Mech. Eng. (1932).

- (17) M. Sanuki and I. Tani. The wall interference of a wind tunnel of elliptic cross-section. *Proc. Phys. Math. Soc. of Japan*, 14, p. 592 (1932).
- (18) R. Seiferth. Untersuchung von Flugzeugmodellen im Windkanal. *Handbuch der Experimentalphysik*, Vol. 4, Part 2, p. 162 (1932).
- (19) L. Rosenhead. The aerofoil in a wind tunnel of elliptic section. *Proc. Roy. Soc.*, A.140, p. 579 (1933).
- (20) L. Rosenhead. Interference due to the walls of a wind tunnel. *Proc. Roy. Soc.*, A. 142, p. 308 (1933).

PART 2

Wings, Two Dimensions

- (21) L. Prandtl. Der Einfluss des Kennwertes auf die Luftkräfte von Tragflügeln. *Ergebnisse der Aerodynamischen Versuchsanstalt zu Göttingen*, Vol. 1, p. 54 (1920).
- (22) H. Glauert. The elements of aerofoil and airscrew theory (1926).
- (23) T. Sasaki. On the effect of the wall of a wind tunnel upon the lift coefficient of a model. *Tokyo Imp. Univ., Aero. Res. Inst., Report 46* (1928).
- (24) Th. von Karman. Beitrag zur Theorie des Auftriebes. *Vorträge aus den Gebieten der Aerodynamik und verwandter Gebiete (Aachen)*, p. 95 (1929).
- (25) L. Rosenhead. The lift of a flat plate between parallel walls. *Proc. Roy. Soc.*, A.132, p. 127 (1931).

PART 3

Symmetrical Bodies

- (26) J. R. Pannel and N. R. Campbell. The variation of the resistance of rigid airship models with the scale and wind speed. *A.R.C., R. & M. 302* (1916).
- (27) J. R. Pannel, R. Jones and G. N. Pell. Experiments in a wind channel on elongated bodies of approximately streamline form. *A.R.C., R. & M. 564* (1918).
- (28) M. M. Munk. Some new aerodynamical relations. *N.A.C.A. Report 114* (1921).
- (29) H. Lamb. On the effect of the walls of an experimental tank on the resistance of a model. *A.R.C., R. & M. 1010* (1926).
- (30) H. Glauert. The characteristics of a Karman vortex street in a channel of finite breadth. *A.R.C., R. & M. 1151* (1927).
- (31) H. Glauert. The effect of a static pressure gradient on the drag of a body tested in a wind tunnel. *A.R.C., R. & M. 1158* (1928).
- (32) G. I. Taylor. The force acting on a body placed in a curved and converging stream of fluid. *A.R.C., R. & M. 1166* (1928).
- (33) A. Fage. On the two-dimensional flow past a body of symmetrical cross-section mounted in a channel of finite breadth. *A.R.C., R. & M. 1223* (1929).
- (34) C. N. H. Lock. The interference of a wind tunnel on a symmetrical body. *A.R.C., R. & M. 1275* (1929).
- (35) G. N. Watson. The use of series of Bessel functions in problems connected with cylindrical wind tunnels. *Proc. Roy. Soc.*, A.130, p. 29 (1930).

- (36) C. N. H. Lock and F. C. Johansen. Wind tunnel interference on streamline bodies. *A.R.C., R. & M. 1451* (1931).
- (37) H. Glauert. The interference of a wind tunnel on a symmetrical body. *A.R.C., R. & M. 1514* (1933).

PART 4

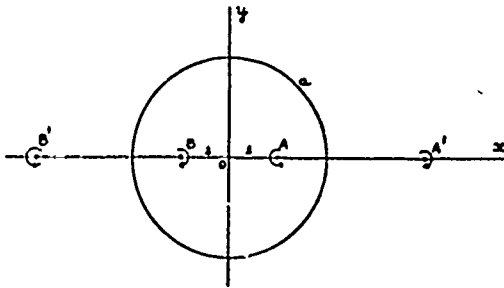
Airscrews

- (38) F. H. Bramwell, E. F. Relf and L. W. Bryant. Experiments to determine the lateral force on a propeller in a side wind. *A.R.C., R. & M. 123* (1914).
- (39) W. F. Durand. Experimental research on air propellers. *N.A.C.A. Report 14* (1917).
- (40) R. McK. Wood and R. G. Harris. Some notes on the theory of an airscrew working in a wind channel. *A.R.C., R. & M. 662* (1920).
- (41) A. Fage, C. N. H. Lock, H. Bateman, and D. H. Williams. Experiments with a family of airscrews, including the effect of tractor and pusher bodies, Part 2. *A.R.C., R. & M. 830* (1922).
- (42) C. N. H. Lock and H. Bateman. The effect of wind tunnel interference on a combination of airscrew and tractor body. *A.R.C., R. & M. 919* (1924).
- (43) H. Glauert and C. N. H. Lock. On the advantages of an open jet type of wind tunnel for airscrew tests. *A.R.C., R. & M. 1033* (1926).
- (44) H. C. H. Townend and J. H. Warsap. Tests of a metal airscrew in a closed tunnel for comparison with American tests in an open jet tunnel. *A.R.C., R. & M. 1137* (1927).
- (45) C. N. H. Lock and F. C. Johansen. Pressure plotting a streamline body with tractor airscrew running. *A.R.C., R. & M. 1230* and *R. & M. 1284* (1929).

R.S.M. 1566.

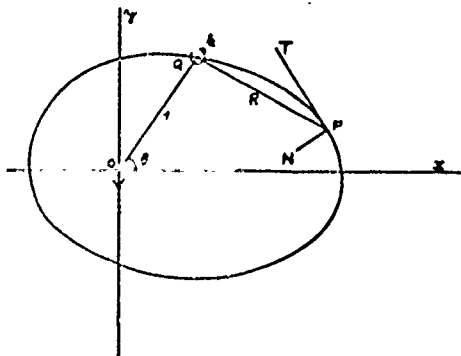
FIG. 3.

WING IN CIRCULAR TUNNEL



SWA WING IN ANY TUNNEL

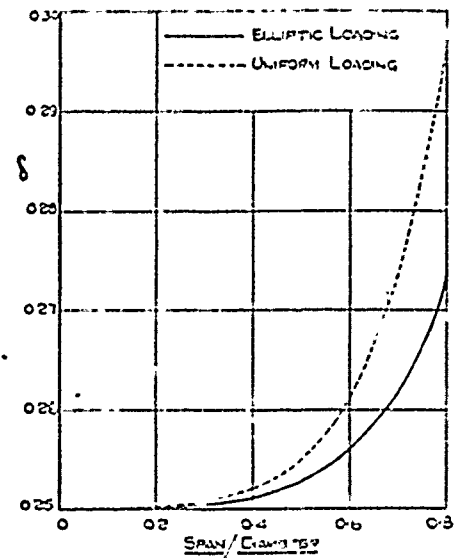
FIG. 4.



R.S.M. 1566.

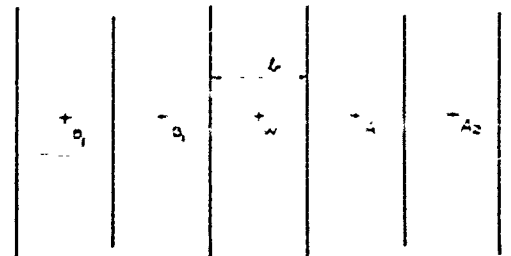
CIRCULAR TUNNEL

FIG. 5.



VERTICAL WALLS

FIG. 6.



R. & M. 1566.

FIG. 7.

RECTANGULAR TUNNELS

(1) CLOSED TUNNEL

+	+	+	+	
-	-	-	-	
+	+ ^w	+	+	
-	-	-	-	
+	+	+	+	h
				l

(2) FREE JET

-	+	-	+	
-	+	-	+	
-	+ ^w	-	+	
-	+	-	+	
-	+	-	+	h
				l

R. & M. 1566.

FIG. 8.

RECTANGULAR TUNNELS

(3) RIGID FLOOR AND ROOF

+	-	+	-	
-	+ ^w	-	+	
+	-	+	-	
-	+	-	+	h
				l

(4) RIGID SIDES

+	+	+	+	
+	+ ^w	+	+	
+	+	+	+	
+	+	+	+	h
				l

(5) RIGID FLOOR

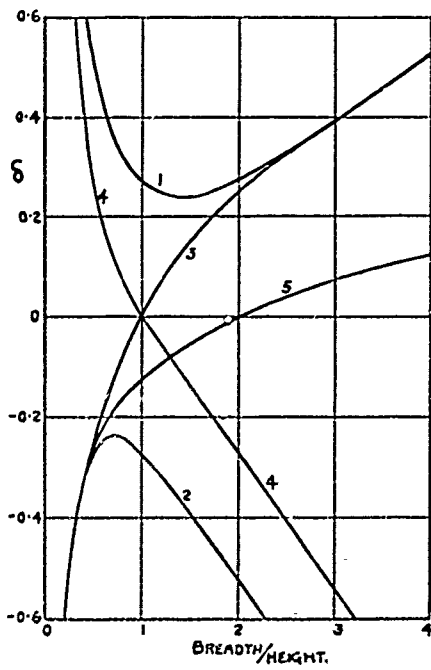
-	+	-	+	
-	+ ^w	-	+	
+	-	+	-	
+	-	+	-	
-	+	-	+	h
				l

R & M. 1566.

FIG. 9.

SMALL WINGS IN RECTANGULAR TUNNELS.

- (1) CLOSED TUNNEL.
- (2) FREE JET.
- (3) RIGID FLOOR AND ROOF.
- (4) RIGID SIDES.
- (5) RIGID FLOOR.

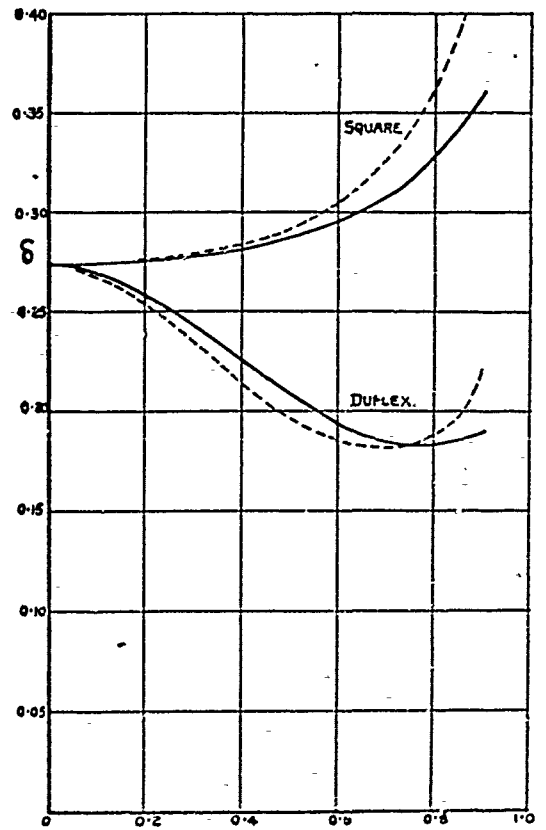


R & M. 1566.

FIG. 10.

CLOSED RECTANGULAR TUNNELS

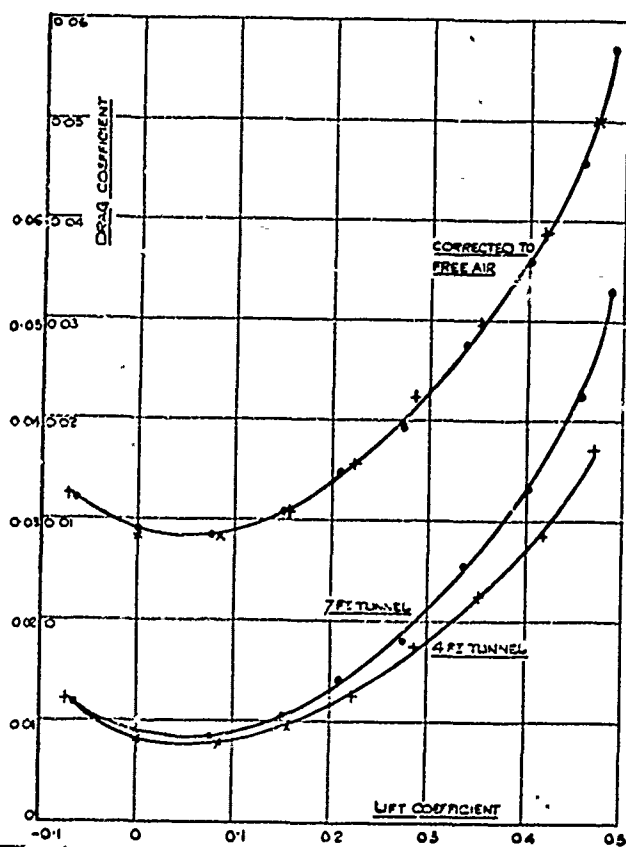
- UNIFORM LOADING.
- ELLIPTIC LOADING.



R.&M. 1566.

FIG 11

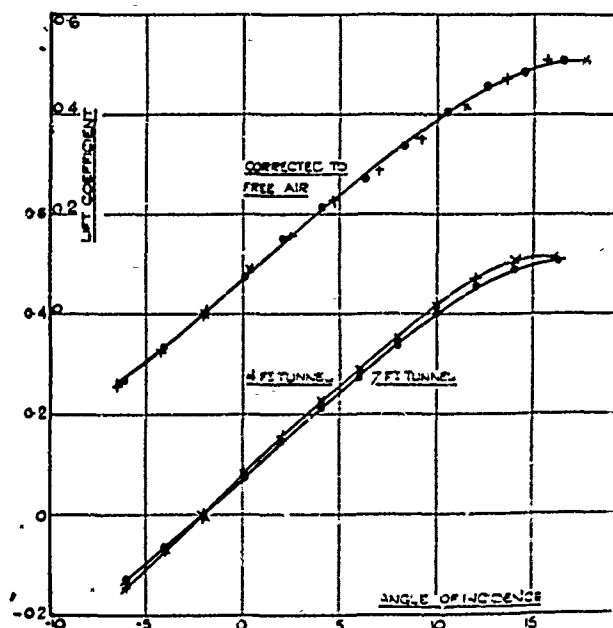
EXPERIMENTAL RESULTS IN SQUARE TUNNELS.



R.&M. 1566.

FIG 12

EXPERIMENTAL RESULTS IN SQUARE TUNNELS.



R. & M. 1566

FIG 14

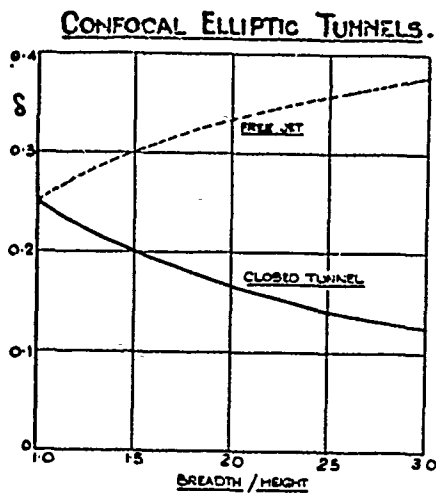
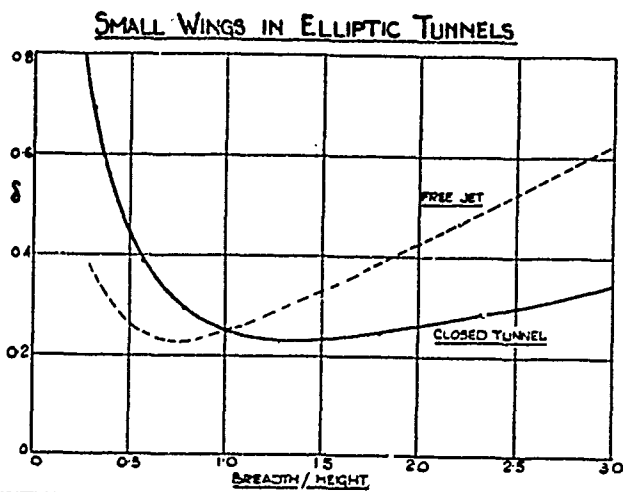


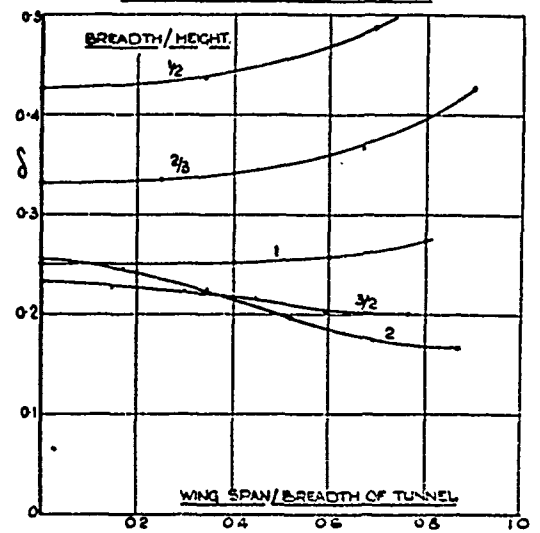
FIG 14.



R. & M. 1566

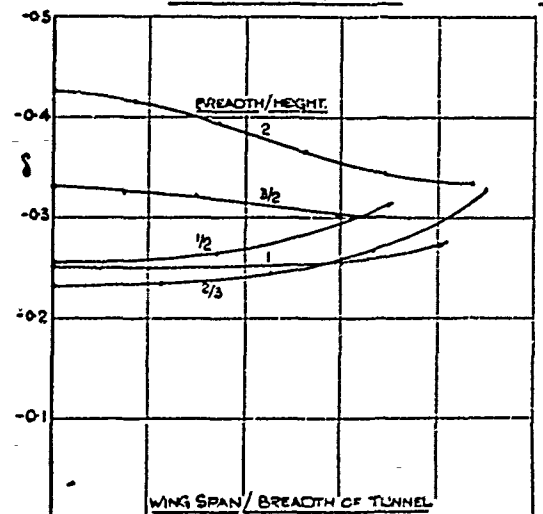
FIG 15.

CLOSED ELLIPTIC TUNNELS



FREE ELLIPTIC JETS

FIG 16



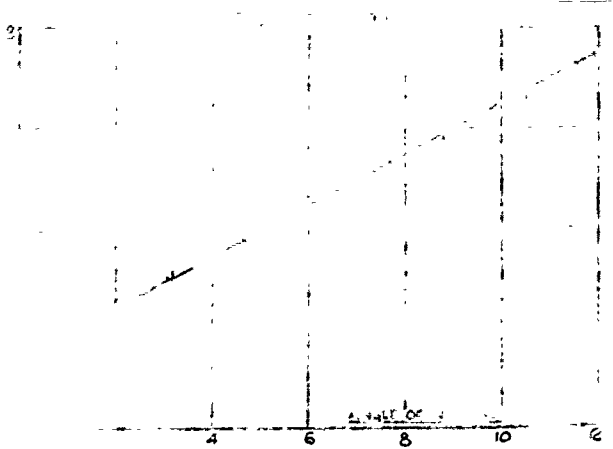
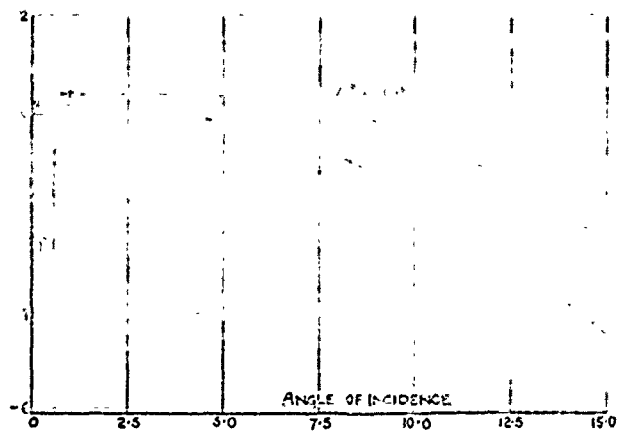
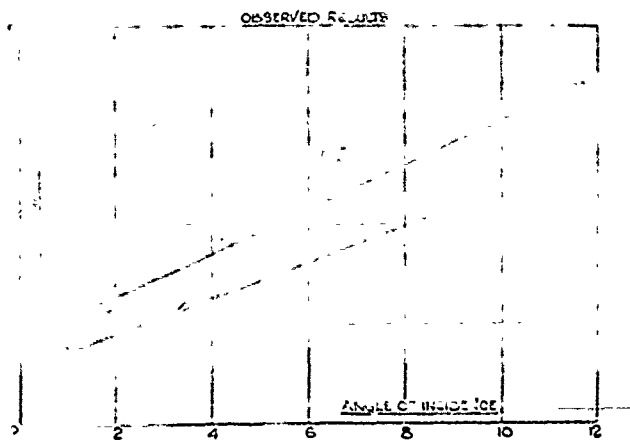
M. 1596.

FIG. 17.

11. 11. 1915

11. 11. 1915

11. 11. 1915



73 M. 1566

FIG. 19

MAXIMUM LIFT COEFFICIENT
IN CLOSED RECTANGULAR TUNNELS

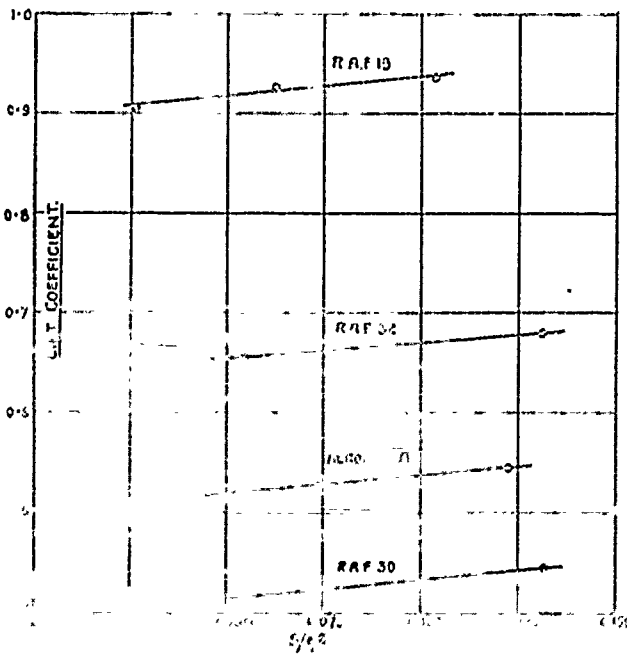


FIG 20

INDUCED FLOW.

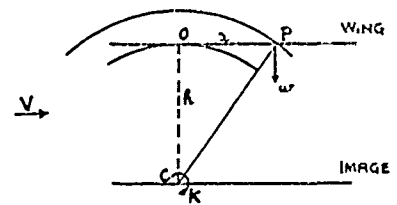
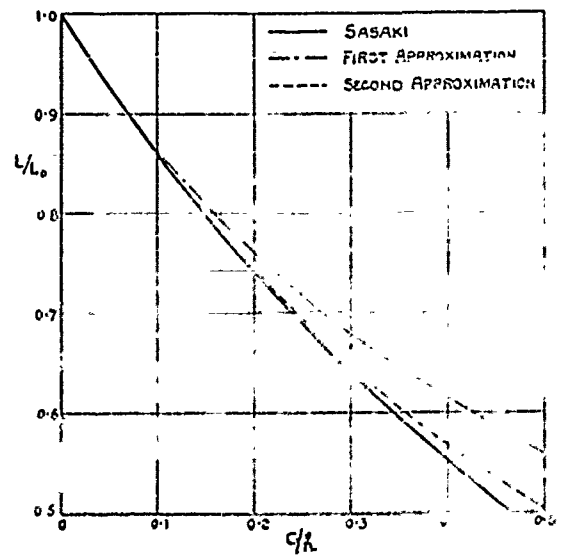


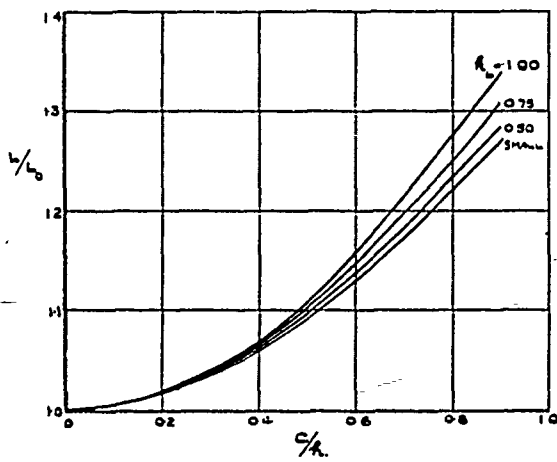
FIG 21

FREE JET.



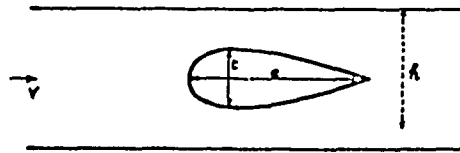
CLOSED TUNNEL.

FIG 22.



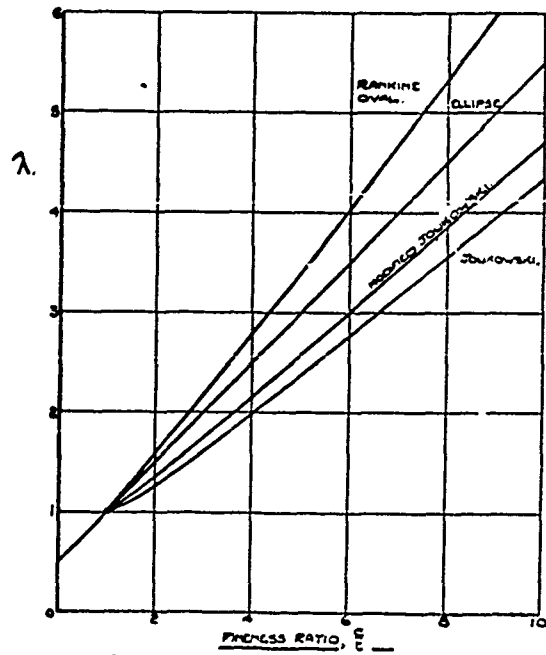
SYMMETRICAL BODY IN A CHANNEL.

FIG 24.



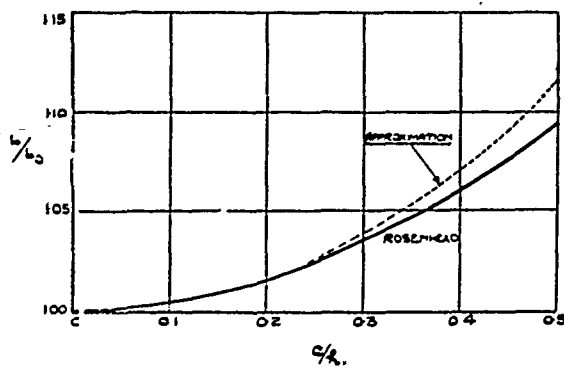
VALUES OF λ .

FIG 25.



CLOSED TUNNEL.

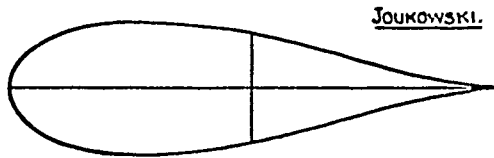
FIG 23.



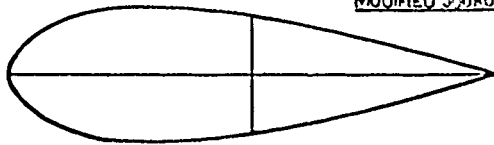
R. & M. 1566.

FIG. 26

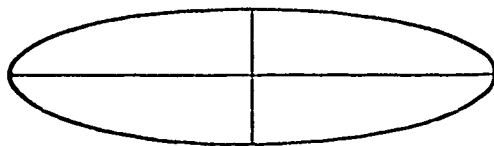
BODY SHAPES



JOUKOWSKI.



MODIFIED JOUKOWSKI.



ELLIPSE.



RANKINE OVAL.

R. & M. 1566.

FIG. 27.

DISCONTINUOUS FLOW

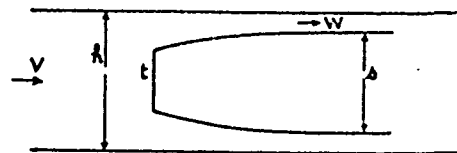
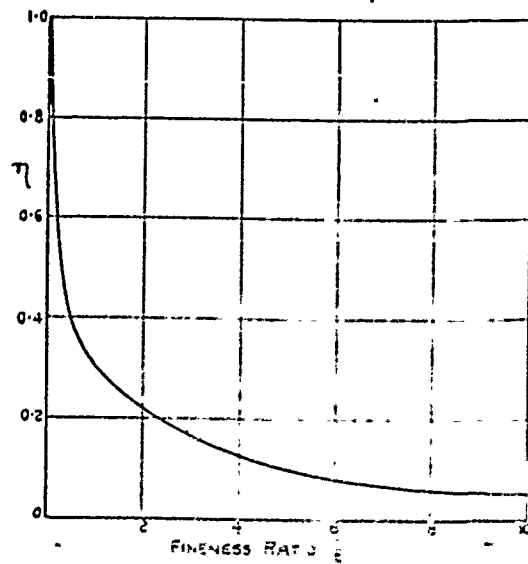


FIG. 28

VALUES OF η



JOUKOWSKI SECTION.

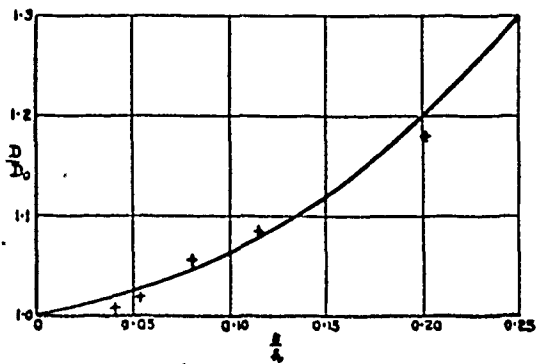
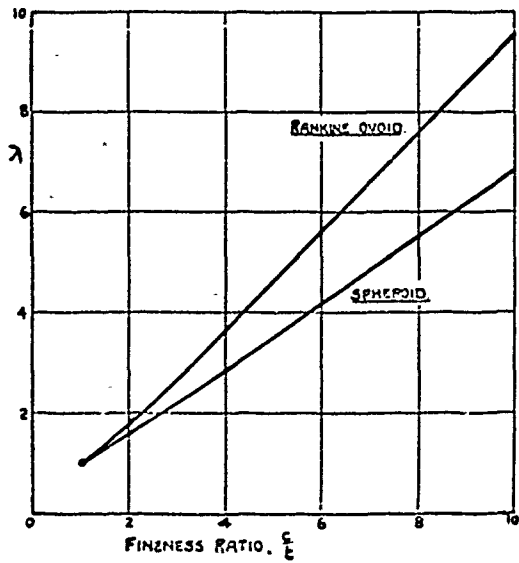


FIG. 30.

VALUES OF λ



R. & M. 1566

FIG. 31.

PRESSURE GRADIENT CORRECTION.

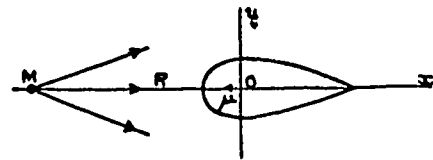
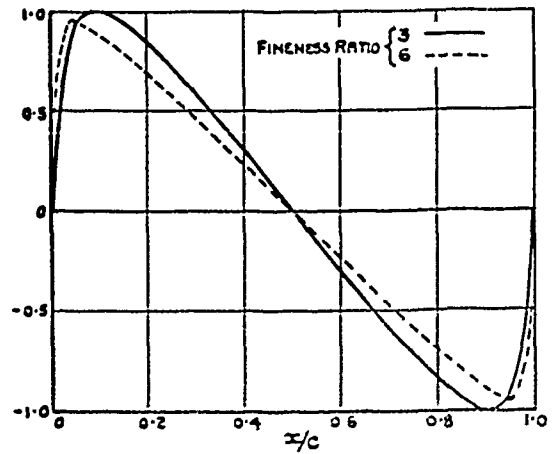


FIG. 32.

PRESSURE GRADIENT FACTOR.



R & M. 1566.

FIG 33.

AIRCREW IN CLOSED TUNNEL.

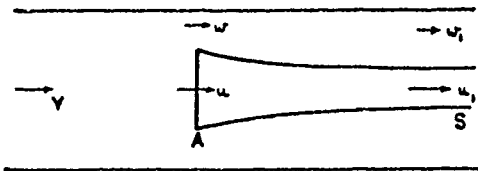


FIG 34.

EQUIVALENT FREE AIRSPEED.

